Protein-coding variation and introgression of regulatory alleles drive plumage pattern diversity in the rock pigeon

Anna I. Vickrey[a], Rebecca Bruders[a], Zev Kronenberg[b], Emma Mackey[a], Ryan J. Bohlender[c], Emily T. Maclary[a], E.J. Osborne[b], Kevin P. Johnson[d], Chad D. Huff[c], Mark Yandell[b], Michael D. Shapiro[a,1]

[a] Department of Biology, University of Utah, Salt Lake City, UT 84112

[b] Department of Human Genetics, University of Utah, Salt Lake City, UT 84112

[c] Department of Epidemiology, M.D. Anderson Cancer Center, University of Texas, Houston, TX 77030

[d] Illinois Natural History Survey, Prairie Research Institute, University of Illinois Urbana-Champaign, Champaign, IL 61820

[1] To whom correspondence should be addressed: shapiro@biology.utah.edu

ABSTRACT

Birds and other vertebrates display stunning variation in pigmentation patterning, yet the genes controlling this diversity remain largely unknown. Rock pigeons (*Columba livia*) are fundamentally one of four color pattern phenotypes, in decreasing order of melanism: T-check, checker, bar (ancestral), or barless. Using whole-genome scans, we identified *NDP* as a candidate gene for this variation. Allele-specific expression differences in *NDP* indicate *cis*-regulatory differences between ancestral and melanistic alleles. Sequence comparisons suggest that derived alleles originated in the speckled pigeon (*Columba guinea*), providing a striking example of introgression of alleles that are favored by breeders and are potentially advantageous in the wild. In contrast, barless rock pigeons have an increased incidence of vision defects and, like two human families with hereditary blindness, carry start-codon mutations in *NDP*. In summary, we find unexpected links between color pattern, introgression, and vision defects associated with regulatory and coding variation at a single locus.

INTRODUCTION

Vertebrates have evolved a vast array of epidermal colors and color patterns in response to natural, sexual, and artificial selection. Numerous studies have identified key genes that determine variation in the types of pigments that are produced (e.g., Hubbard et al. 2010; Manceau et al. 2010; Roulin and Ducrest 2013; Domyan et al. 2014; Rosenblum et al. 2014). In contrast, considerably less is known about the genetic mechanisms that determine pigment *patterning* throughout the entire epidermis and within individual epidermal appendages (e.g., feathers, scales, and hairs) (Kelsh 2004; Protas and Patel 2008; Kelsh et al. 2009; Lin et al. 2009; Kaelin et al. 2012; Lin et al. 2013; Eom et al. 2015; Poelstra et al. 2015; Mallarino et al. 2016). In birds, color patterns are strikingly diverse among different populations and species, and these traits have profound impacts on mate-choice, crypsis, and communication (Hill and McGraw 2006).

The domestic rock pigeon (*Columba livia*) displays enormous phenotypic diversity within and among over 350 breeds, including a wide variety of plumage pigmentation patterns (Shapiro and Domyan 2013; Domyan and Shapiro 2017). Some of these pattern phenotypes are found in feral and wild populations as well (Johnston and Janiga 1995). A large number of genetic loci contribute to pattern variation in rock pigeons, including genes that contribute in an additive fashion and others that epistatically mask the effects of other loci (Jones 1922; Hollander 1937; Sell 2012; Domyan et al. 2014). Despite the genetic complexity of the full spectrum of plumage pattern diversity in pigeons, classical genetic experiments demonstrate that major wing shield pigmentation phenotypes are determined by an allelic series at a single locus (*C*,

for "checker" pattern) that produces four phenotypes: T-check (C^T allele, also called T-pattern), checker (*C*), bar (+), and barless (*c*), in decreasing order of dominance and melanism (Fig. 1A) (Bonhote and Smalley 1911; Hollander 1938; Hollander 1983; Levi 1986; Sell 2012). Bar is the ancestral phenotype (Darwin 1859, 1868), yet checker and T-check can occur at higher frequencies than bar in urban feral populations, suggesting a fitness advantage in areas of dense human habitation (Obukhova and Kreslavskii 1984; Johnston and Janiga 1995; Čanády and Mošanský 2013).

Color pattern variation is associated with several important life history traits in feral pigeon populations. For example, checker and T-check birds have higher frequencies of successful fledging from the nest, longer (up to year-round) breeding seasons, and can sequester more toxic heavy metals in plumage pigments through chelation (Petersen and Williamson 1949b; Lofts et al. 1966; Murton et al. 1973; Chatelain et al. 2014; Chatelain et al. 2016). Relative to bar, checker and T-check birds also have reduced fat storage and, perhaps as a consequence, lower overwinter adult survival rates in harsh rural environments (Petersen and Williamson 1949a; Jacquin et al. 2012). Disassortative mating occurs in feral pigeons with different patterns, so sexual selection probably influences the frequencies of wing pigmentation patterns in feral populations as well (Burley 1981; Johnston and Johnson 1989). In contrast, barless, the recessive and least melanistic phenotype, is rarely observed in feral pigeons (Johnston and Janiga 1995). In domestic populations, barless birds have a higher frequency of vision defects, sometimes referred to as "foggy" vision (Hollander and Miller 1981; Hollander 1983; Mangile 1987), which could negatively impact fitness in the wild.

74 In this study, we investigate the molecular and evolutionary mechanisms
75 underlying wing pattern diversity in pigeons. We discover both coding and regulatory
76 variation at a single candidate gene, and a trans-species polymorphism linked with
77 pattern variation within and between species that likely resulted from interspecies
78 hybridization.
79
80 **RESULTS AND DISCUSSION**
81 **A genomic region on Scaffold 68 is associated with wing pattern phenotype**
82 To identify the genomic region containing the major wing pigmentation pattern
83 locus, we used a probabilistic measure of allele frequency differentiation (pFst; Domyan
84 et al. 2016) to compare the resequenced genomes of bar pigeons to genomes of pigeons
85 with either checker or T-check patterns (see Methods). Checker and T-check birds were
86 grouped together because these two patterns are sometimes difficult to distinguish, even
87 for experienced hobbyists (Fig. 1A). Checker birds are typically less pigmented than T-
88 check birds, but genetic modifiers of pattern phenotypes can minimize this difference. A
89 two-step whole-genome scan (see Methods, Fig. 1B, Fig. S1A) identified a single ~103-
90 kb significantly differentiated region on Scaffold 68 that was shared by all checker and T-
91 check birds (position 1,702,691-1,805,600 of the Cliv_1.0 pigeon genome assembly
92 (Shapiro et al. 2013); p = 1.11e-16, genome-wide significance threshold = 9.72e-10). The
93 minimal shared region was defined by haplotype breakpoints in a homozygous checker
94 and a homozygous bar bird and is hereafter referred to as the minimal checker haplotype.
95 As expected for the well-characterized allelic series at the *C* locus, we also found that a
96 broadly overlapping region of Scaffold 68 was highly differentiated between the genomes

of bar and barless birds (p = 3.11e-15, genome-wide significance threshold = 9.71e-10; Fig. S1B). Together, whole-genome comparisons identified a single genomic region corresponding to the wing pattern *C* locus.

A copy number variant is associated with melanistic wing patterns

To identify genetic variants associated with the derived checker and T-check phenotypes, we first compared annotated protein-coding genes throughout the genome. We found a single, predicted, fixed change in EFHC2 (Y572C, Fig. S2) in checker and T-check birds relative to bar birds (VAAST; Yandell et al. 2011). However, this same amino acid substitution is also found in *Columba rupestris*, a closely related species to *C. livia* that has a bar wing pattern. Thus, the Y572C substitution is not likely to be causative for the checker or T-check pattern, nor is it likely to have a strong impact on protein function (MutPred2 score 0.468, no recognized affected domain; PolyPhen-2 score 0.036; Adzhubei et al. 2010; Pejaver et al. 2017).

Next, we examined sequence coverage across the checker haplotype and discovered a copy number variable (CNV) region (approximate breakpoints at Scaffold 68 positions 1,790,000 and 1,805,600). Based on normalized read-depths of resequenced birds, we determined that the CNV region has one, two, or four copies per chromosome. Bar birds (n=12) in our resequencing panel always had a total of two copies in the CNV region (one on each chromosome), but most checker (n=5 of 7) and T-check (n=2 of 2) genomes examined had additional copies of the CNV (Fig. 2A). Using a PCR assay to amplify across the breakpoints in birds with more than one copy per chromosome, we determined that additional copies result from tandem repeats. We found no evidence that

120 the checker haplotype contains an inversion based on mapping of paired-end reads at the
121 CNV breakpoints (WHAM; Kronenberg et al. 2015). In addition, we were able to amplify
122 unique PCR products that span the outer CNV breakpoints (data not shown), suggesting
123 that there are no inversions within the CNV region.

124 The fact that some checker birds had only two total copies of the CNV region
125 demonstrates that a copy number increase is not necessary to produce melanistic
126 phenotypes. However, consistent with the dominant inheritance pattern of the phenotype,
127 all checker and T-check birds had at least one copy of the checker haplotype. Thus, a
128 checker haplotype on at least one chromosome appears to be necessary for the dominant
129 melanistic phenotypes, but additional copies of the CNV region are not.

130 In a larger sample of pigeons, we found a significant association between copy
131 number and phenotype (TaqMan assay; pairwise Wilcoxon test, p=2.1e-05). Checker
132 (n=40 of 56) and T-check (n=15 of 18) patterns were associated with additional copies,
133 and pigeons with the bar pattern (n=20) never had more than two copies in total (Fig.
134 2B). Although additional copies of the CNV only occurred in checker and T-check birds,
135 we did not observe a consistent number of copies associated with either phenotype. This
136 could be due to a variety of factors, including modifiers that darken genotypically-
137 checker birds to closely resemble T-check (Jones 1922; Sell 2012) and environmental
138 factors such as temperature-dependent darkening of the wing shield during feather
139 development (Podhradsky 1968).

140 Due to the potential ambiguity in categorical phenotyping, we next measured the
141 percent of pigmented area on the wing shield and tested for associations between copy
142 number and percentage of pigmented wing shield area. We phenotyped and genotyped an

143 additional 63 birds from diverse domestic breeds as well as 26 feral birds, and found that
144 estimated copy number in the variable region was correlated with the amount of dark
145 pigment on the wing shield (nonlinear least squares regression, followed by r^2
146 calculation; r^2=0.46) (Fig. 2C). This correlation was a better fit to the regression when
147 ferals were excluded (r^2=0.68, Fig. S3B), possibly because numerous pigmentation
148 modifiers (e.g., *sooty* and *dirty*) are segregating in feral populations (Hollander 1938;
149 Johnston and Janiga 1995). Together, our analyses of genetic variation among
150 phenotypes point to a CNV that is associated with qualitative and quantitative color
151 pattern variation in pigeons.
152
153 **_NDP_ is differentially expressed in feather buds of different wing pattern phenotypes**
154 The CNV that is associated with wing pattern variation resides between two
155 genes, *EFHC2* and *NDP*. *EFHC2* is a component of motile cilia, and mouse mutants have
156 juvenile myoclonic epilepsy (Linck et al. 2014). In humans, allelic variation in *EFHC2* is
157 also associated with differential fear responses and social cognition (Weiss et al. 2007;
158 Blaya et al. 2009; Startin et al. 2015; but see Zinn et al. 2008). However, *EFHC2* has not
159 been implicated in pigmentation phenotypes in any organism. *NDP* encodes a secreted
160 ligand that activates *WNT* signaling by binding to its only known receptor FZD4 and its
161 co-receptor LRP5 (Smallwood et al. 2007; Hendrickx and Leyns 2008; Deng et al. 2013;
162 Ke et al. 2013). Notably, *NDP* is one of many differentially expressed genes in the
163 feathers of closely related crow subspecies that differ, in part, by the intensity of plumage
164 pigmentation (Poelstra et al. 2015). Furthermore, FZD4 is a known melanocyte stem cell
165 marker (Yamada et al. 2010). Thus, based on expression variation in different crow

166 plumage phenotypes, and the expression of its receptor in pigment cell precursors, *NDP*
167 is a strong candidate for pigment variation in pigeons.

168 The CNV in the intergenic space between *EFHC2* and *NDP* in the candidate
169 region, coupled with the lack of candidate coding variants between bar and checker
170 haplotypes, led us to hypothesize that the CNV region might contain regulatory variation
171 that could alter expression of one or both neighboring genes. To test this possibility, we
172 performed qRT-PCR on RNA harvested from regenerating wing shield feathers of bar,
173 checker, and T-check birds. *EFHC2* was not differentially expressed between bar and
174 either checker or T-check patterned feathers (p=0.19, pairwise Wilcoxon test, p-value
175 adjustment method: fdr), although expression levels differed slightly between the checker
176 and T-check patterned feathers (p=0.046, Fig. 3A). Expression levels of other genes
177 adjacent to the minimal checker haplotype region also did not vary by phenotype (Fig.
178 S4).

179 In contrast, expression of *NDP* was significantly increased in checker feathers –
180 and even higher in T-check feathers – relative to bar feathers (Fig. 3A) (bar-checker
181 comparison, p=1.9e-05; bar-T-check, p=1.0e-08; checker-T-check, p=0.0071; pairwise
182 Wilcoxon test, all comparisons were significant at a false discovery rate of 0.05).
183 Moreover, when qRT-PCR expression data for checker and T-check feathers were
184 grouped by copy number instead of categorical phenotype, the number of CNV copies
185 was positively associated with *NDP* expression level (Fig. S5). Thus, expression of *NDP*
186 is positively associated with both increased melanism (categorical pigment pattern
187 phenotype) and CNV genotype.

188 The increase in *NDP* expression could be the outcome of at least two molecular
189 mechanisms. First, one or more regulatory elements in the CNV region (or elsewhere)
190 could increase expression of *NDP* in *cis*. Such changes would only affect expression of
191 the allele on the same chromosome (Wittkopp et al. 2004). Second, *trans*-acting factors
192 encoded within the minimal checker haplotype (e.g., *EFHC2* or an unannotated feature)
193 could increase *NDP* expression, resulting in an upregulation of *NDP* alleles on both
194 chromosomes.

195 To distinguish between these possibilities, we carried out allele-specific
196 expression assays (Domyan et al. 2014; Domyan et al. 2016) on the regenerating feathers
197 of birds that were heterozygous for bar and checker alleles in the candidate region
198 (checker alleles with one, two, or four copies of the CNV). In the common *trans*-acting
199 cellular environment of heterozygous birds, checker alleles of *NDP* were more highly
200 expressed than bar alleles, and these differences were further amplified in checker alleles
201 with more copies of the CNV (Fig. 3B) ($p=0.0028$ for two-sample t-test between 1 vs. 4
202 copies, $p=1.84e-06$ for generalized linear model regression). In comparison, transcripts of
203 *EFHC2* from checker and bar alleles were not differentially expressed in the hybrid
204 background (Fig. 3B) ($p=0.5451$ for two-sample t-test between 1 vs. 4 copies, $p=0.471$
205 for linear regression). Together, our expression studies indicate that a *cis*-acting
206 regulatory change drives increased expression of *NDP* in pigeons with more melanistic
207 plumage patterns, but does not alter expression of *EFHC2* or other nearby genes (Figs.
208 3A, S4). Furthermore, because *NDP* expression increases with additional copies of the
209 CNV, the regulatory element probably resides within the CNV itself.
210

A missense mutation at the start codon of *NDP* is associated with barless

In humans, mutations in *NDP* can result in Norrie disease, a recessively-inherited disorder characterized by a suite of symptoms including vision deficiencies, intellectual and motor impairments, and auditory deficiencies (Norrie 1927; Warburg 1961; Holmes 1971; Chen et al. 1992; Sims et al. 1992). Protein-coding mutations in *NDP*, including identical mutations segregating within single-family pedigrees, result in variable phenotypic outcomes, including incomplete penetrance (Meindl et al. 1995; Berger 1998; Allen et al. 2006). Intriguingly, barless pigeons also have an increased incidence of vision deficiencies and, as in humans with certain mutant alleles of *NDP*, this phenotype is not completely penetrant (Hollander 1983). Thus, based on the known allelism at the *C* locus, the nomination of regulatory changes at *NDP* as candidates for the *C* and C^T alleles, and the vision-related symptoms of Norrie disease, *NDP* is also a strong candidate for the barless phenotype (*c* allele).

To test the prediction that variation in *NDP* is associated with the barless phenotype, we used VAAST to scan the resequenced genomes of 9 barless pigeons and found that all were homozygous for a nonsynonymous protein-coding change at the start codon of *NDP* that was perfectly associated with the barless wing pattern phenotype. We detected no other genes with fixed coding changes or regions of significant allele frequency differentiation (pFst) elsewhere in the genome. We genotyped an additional 14 barless birds and found that all were homozygous for the same start-codon mutation (Fig. S6). The barless mutation is predicted to truncate the amino terminus of the NDP protein by 11 amino acids, thereby disrupting the 24-amino acid signal peptide sequence (www.uniprot.org, Q00604 NDP_Human). *NDP* is still transcribed and detectable by RT-

PCR in regenerating barless feathers (data not shown); therefore, we speculate that the start-codon mutation might alter the normal secretion of the protein into the extracellular matrix (Gierasch 1989).

In humans, coding mutations in *NDP* are frequently associated with a suite of neurological deficits. In pigeons, however, only wing pigment depletion and vision defects are reported in barless homozygotes. Remarkably, two human families segregating Norrie disease have only vision defects, and like barless pigeons, these individuals have start-codon mutations in *NDP* (Fig. S6) (Isashiki et al. 1995). Therefore, signal peptide mutations might affect a specific subset of developmental processes regulated by *NDP*, while leaving other (largely neurological) functions intact. In summary, wing pattern phenotypes in pigeons are associated with the evolution of both regulatory (checker, T-check) and coding (barless) changes in the same gene, and barless pigeons share a partially-penetrant visual deficiency with human patients who have start-codon substitutions.

Signatures of introgression of the checker haplotype

Pigeon fanciers have long hypothesized that the checker pattern in the rock pigeon (*Columba livia*) resulted from a cross-species hybridization event with the speckled pigeon (*Columba guinea,* Fig. S7), a species with a checker-like wing pattern (G. Hochlan, G. Young, personal communication) (Hollander 1983). Although *C. livia* and *C. guinea* diverged an estimated 4-5 million years ago, inter-species crosses can produce fertile hybrids (Whitman 1919; Irwin et al. 1936; Taibel 1949; Miller 1953). Moreover, hybrid F_1 and backcross progeny between *C. guinea* and bar *C. livia* have checkered

257 wings, much like *C. livia* with the *C* allele (Whitman 1919; Taibel 1949). Taibel (1949)
258 showed that, although hybrid F_1 females were infertile, two more generations of
259 backcrossing to *C. livia* could produce checker offspring of both sexes that were fully
260 fertile. In short, Taibel introgressed the checker trait from *C. guinea* into *C. livia* in just
261 three generations.

262 To evaluate the possibility of an ancient cross-species introgression event, we
263 sequenced an individual *C. guinea* genome to ~30X coverage and mapped the reads to
264 the *C. livia* reference assembly. We calculated four-taxon *D*-statistics ("ABBA-BABA"
265 test; Durand et al. 2011) to test for deviations from expected sequence similarity between
266 *C. guinea* and *C. livia*, using a wood pigeon (*C. palumbus*) genome as an outgroup. In
267 this case, the null expectation is that the *C* candidate region will be more similar between
268 conspecific bar and checker *C. livia* than either will be to the same region in *C. guinea*.
269 That is, the phylogeny of the candidate region should be congruent with the species
270 phylogeny. However, we found that the *D*-statistic approaches 1.0 in the candidate region
271 (n=10 each for bar and checker *C. livia*), indicating that checker *C. livia* are more similar
272 to *C. guinea* than to conspecific bar birds in this region (Fig. 4A). The mean genome-
273 wide *D*-statistic was close to zero (0.021), indicating that bar and checker sequences are
274 more similar to each other throughout the genome than either one is to *C. guinea*.

275 This unexpected similarity between *C. guinea* and checker *C. livia* in the pattern
276 candidate region was further supported by sequence analysis using HybridCheck (Ward
277 and van Oosterhout 2016). Outside of the candidate region, checker birds have a high
278 sequence similarity to conspecific bar birds and low similarity to *C. guinea* (Fig. 4B).
279 Within the candidate region, however, this relationship shows a striking reversal, and

checker and *C. guinea* sequences are most similar to each other. In addition, although the genome-wide D-statistic was relatively low, the 95% confidence interval (CI) was greater than zero (0.021 to 0.022), providing further evidence for one or more introgression events from *C. guinea* into checker and T-check genomes. Unlike in many checker and T-check *C. livia*, we did not find additional copies of the CNV region in *C. guinea*. This could indicate that the CNV expanded in *C. livia*, or that the CNV is present in a subset of *C. guinea* but has not yet been sampled. Taken together, these patterns of sequence similarity and divergence support the hypothesis that the candidate checker haplotype in rock pigeons originated by introgression from *C. guinea*.

Estimated divergence time among pattern locus haplotypes

While post-divergence introgression is an attractive hypothesis to explain the sequence similarity between checker *C. livia* and *C. guinea*, another formal possibility is that sequence similarity between these groups is due to incomplete lineage sorting. Therefore, to assess whether the minimal checker haplotype might have been present in the last common ancestor of *C. guinea* and *C. livia*, we measured single nucleotide differences among different alleles of the minimal haplotype and compared these counts to polymorphism rates expected to accumulate over the divergence time between *C. livia* and *C. guinea* (Fig. 4C, purple bar, see Methods).

We found that polymorphisms between bar *C. livia* and *C. guinea* approached the number expected to accumulate in 4-5 MY (1708±109 mean SNPs, Fig. 4C), but so did intraspecific comparisons between bar and checker *C. livia* (1564±99). In contrast, *C. guinea* and *C. livia* checker sequences had only 384±6 mean differences, significantly

303 fewer than would be expected to accumulate between the two species ($p < 2.2e-16$, t-
304 test). These results support an introgression event from *C. guinea* to *C. livia*, rather than a
305 shared ancestral allele inherited from a common ancestor prior to divergence. Among 11
306 checker haplotype sequences we found only 26±8 mean differences.
307 We then estimated the age of the minimal checker haplotype following Voight et
308 al. (2006). Using a recombination rate calculated for rock pigeon (Holt et al. 2017), the
309 minimal checker haplotype is estimated to have been introgressed 857 (95% CI 534 to
310 1432) generations ago. Therefore, assuming 1-2 generations per year in *C. livia*,
311 introgression events likely occurred well after the domestication of rock pigeons (~5000
312 years ago). The ranges of *C. livia* and *C. guinea* overlap in northern Africa (del Hoyo et
313 al. 2017), so introgression events could have occurred in free-living populations.
314 Alternatively, or perhaps additionally, multiple (but relatively similar) checker
315 haplotypes could have been introgressed more recently by pigeon breeders. Once male
316 hybrids are generated, this can be accomplished in just a few generations (Taibel 1949).
317 This explanation is supported by lack of diversity among checker haplotypes, with only
318 26±8 mean differences, which is unusually low for the diversity typically observed in
319 large, free-living pigeon populations (Shapiro et al. 2013). Additional *C. guinea* genome
320 sequences will help to characterize allelic variation at this locus and resolve these
321 possibilities.
322
323 **Introgression and pleiotropy**
324 Adaptive traits can arise through new mutations or standing variation within a
325 species, and a growing number of studies point to cross-species adaptive introgressions

among vertebrates and other animals (Hedrick 2013; Harrison and Larson 2014; Zhang et al. 2016). In some cases, introgressed loci are associated with adaptive traits in the receiving species, including high-altitude tolerance in Tibetan human populations from Denisovans (Huerta-Sanchez et al. 2014), resistance to anticoagulant pesticides in the house mouse from the Algerian mouse (Song et al. 2011; Liu et al. 2015), and beak morphology among different species of Darwin's finches (Lamichhaney et al. 2015). Among domesticated birds, introgressions are responsible for skin and plumage color traits in chickens and canaries, respectively (Eriksson et al. 2008; Lopes et al. 2016). Alleles under artificial selection in a domesticated species can be advantageous in the wild as well, as in the introgression of dark coat color from domestic dogs to wolves (Anderson et al. 2009) (however, color might actually be a visual marker for an advantageous physiological trait conferred by the same allele; Coulson et al. 2011).

In this study, we identified a putative introgression into *C. livia* from *C. guinea* that is advantageous both in artificial (selection by breeders) and free-living urban environments (sexual and natural selection). A change in plumage color pattern is an immediately obvious phenotypic consequence of the checker allele, yet other traits are linked to this pigmentation pattern. For example, checker and T-check pigeons have longer breeding seasons, up to year-round in some locations (Lofts et al. 1966; Murton et al. 1973), and *C. guinea* breeds year-round in most of its native range as well (del Hoyo et al. 2017). Perhaps not coincidentally, *NDP* is expressed in the gonad tissues of adult *C. livia* (MacManes et al. 2017) and the reproductive tract of other amniotes (Paxton et al. 2010). Abrogation of expression or function of *NDP* or its receptor *FZD4* is associated with infertility and gonad defects (Luhmann et al. 2005; Kaloglu et al. 2011; Ohlmann et

al. 2012; Ohlmann and Tamm 2012). Furthermore, checker and T-check birds deposit less fat during normally reproductively quiescent winter months. In humans, expression levels of *FZD4* and the co-receptor *LRP5* in adipose tissue respond to varying levels of insulin (Karczewska-Kupczewska et al. 2016), and *LRP5* regulates the amount and location of adipose tissue deposition (Loh et al. 2015; Karczewska-Kupczewska et al. 2016). Therefore, based on its reproductive and metabolic roles in pigeons and other amniotes, *NDP* is a viable candidate not only for color pattern variation, but also for the suite of other traits observed in free-living (feral and wild) checker and T-check pigeons. Indeed, the potential pleiotropic effects of *NDP* raise the possibility that reproductive output and other physiological advantages are secondary or even primary targets of selection, and melanistic phenotypes are honest genetic signals of a cluster of adaptive traits controlled by a single locus.

Adaptive *cis*-regulatory change is emerging as an important theme in the evolution of vertebrates and other animals (Shapiro et al. 2004; Miller et al. 2007; Chan et al. 2010; Wittkopp and Kalay 2012; O'Brown et al. 2015). In some cases, the evolution of multiple regulatory elements of the same gene can fine-tune phenotypes, such as mouse coat color and trichome distribution in fruit flies (McGregor et al. 2007; Linnen et al. 2013). Cross-species introgression can result in the simultaneous transfer of multiple advantageous traits (Rieseberg 2011), and the potential role of *NDP* in both plumage and physiological variation in pigeons could represent a striking example of this process.

Wing pigmentation patterns that resemble checker are present in many wild species within and outside of Columbidae including *Patagioenas maculosa* (Spot-winged pigeon), *Spilopelia chinensis* (Spotted dove), *Geopelia cuneata* (Diamond dove), *Gyps*

372 *rueppelli* (Rüppell's vulture), and *Pygiptila stellaris* (Spot-winged antshrike). Based on
373 our results in pigeons, *NDP* and its downstream targets can serve as initial candidate
374 genes to ask whether similar molecular mechanisms generate convergent patterns in other
375 species.
376
377 **MATERIALS & METHODS**
378 **Ethics statement**
379 Animal husbandry and experimental procedures were performed in accordance
380 with protocols approved by the University of Utah Institutional Animal Care and Use
381 Committee (protocols 10-05007, 13-04012, and 16-03010).
382
383 **DNA sample collection and extraction**
384 Blood samples were collected in Utah at local pigeon shows, at the homes of local
385 pigeon breeders, from pigeons in the Shapiro lab, and from ferals that had been captured
386 in Salt Lake City, Utah. Photos of each bird were taken upon sample collection for our
387 records and for phenotype verification. Tissue samples of *C. rupestris*, *C. guinea*, and *C.*
388 *palumbus* were provided by the University of Washington Burke Museum, Louisiana
389 State University Museum of Natural Science, and Tracy Aviary, respectively. Breeders
390 outside of Utah were contacted by email or phone to obtain feather samples. Breeders
391 were sent feather collection packets and instructions, and feather samples were sent back
392 to the University of Utah along with detailed phenotypic information. Breeders were
393 instructed to submit only samples that were unrelated by grandparent. DNA was then
394 extracted from blood, tissue, and feathers as previously described (Stringham et al. 2012).

395

396 **Determination of color and pattern phenotype of adult birds**

397 Feather and color phenotypes of birds were designated by their respective
398 breeders. Birds that were raised in our facility at the University of Utah or collected from
399 feral populations were assigned a phenotype using standard references (Levi 1986; Sell
400 2012).

401

402 **Genomic Analyses**

403 BAM files from a panel of previously resequenced birds were combined with
404 BAM files from 8 additional barless birds, 23 bar and 23 checker birds (22 feral, 24
405 domestics), a single *C. guinea*, and a single *C. palumbus*. SNVs and small indels were
406 called using the Genome Analysis Toolkit (Unified Genotyper and LeftAlignAnd
407 TrimVariants functions, default settings) (McKenna et al. (2010) *Genome Research).*
408 Variants were filtered as described previously (Domyan et al. 2016) and the subsequent
409 variant call format (VCF) file was used for pFst and ABBA-BABA analyses as part of
410 the VCFLIB software library (https://github.com/vcflib) and VAAST (Yandell et al.
411 2011) as described previously (Shapiro et al. 2013).

412 pFst was first performed on whole-genomes of 32 bar and 27 checker birds. Some
413 of the checker and bar birds were sequenced to very low coverage (~1X), so we were
414 unable to confidently define the boundaries of the shared haplotype. To remedy this
415 issue, we used the core of the haplotype to identify additional bar and checker birds from
416 a set of birds that had already been sequenced to higher coverage (Shapiro et al. 2013).
417 These additional birds were not included in the initial scan because their wing pattern

418 phenotypes were concealed by other color and pattern traits that are epistatic to bar and
419 check phenotypes. For example, the recessive red (*e*) and spread (*S*) loci produce a
420 uniform pigment over the entire body, thereby obscuring any bars or checkers (Jones
421 1922; Hollander 1938; Sell 2012; Domyan et al. 2014). Although the major wing pattern
422 is not visible in these birds, the presence or absence of the core checker haplotype
423 allowed us to characterize them as either bar or checker/T-check. We then re-ran pFst
424 using 17 bar and 24 checker/T-check birds with at least 8X mean read depth coverage
425 and (Fig. 1B), and found a minimal shared checker haplotype of ~100 kb (Scaffold 68
426 position 1,702,691-1,805,600), as defined by haplotype breakpoints in a homozygous
427 checker and a homozygous bar bird (NCBI BioSamples SAMN01057561 and
428 SAMN01057543, respectively; BioProject PRJNA167554). pFst was also used to
429 compare the genomes of 32 bar and 9 barless birds. New sequence data for *C. livia* are
430 deposited in the NCBI SRA database under BioProject PRJNA428271 with the
431 BioSample accession numbers SAMN08286792- SAMN08286844. (Submission of
432 sequences for *C. guinea* and *C. palumbus* is in progress.)
433
434 **CNV breakpoint identification and read depth analysis**
435 The approximate breakpoints of the CNV region were identified at Scaffold 68
436 positions 1,790,000 and 1,805,600 using WHAM in resequenced genomes of
437 homozygous bar or checker birds with greater than 8x coverage (Kronenberg et al. 2015).
438 For 12 bar, 7 checker, and 2 T-check resequenced genomes, Scaffold 68 gdepth files
439 were generated using VCFtools (Danecek et al. 2011). Two subset regions were
440 specified: the first contained the CNV and the second was outside of the CNV and was

441 used for normalization (positions 1,500,000-2,000,000 and 800,000-1,400,000,
442 respectively). Read depth in the CNV was normalized by dividing read depth by the
443 average read depth from the second (non-CNV) region, then multiplying by two to
444 normalize for diploidy.
445
446 **Taqman assay for copy number variation**
447 Copy number variation was estimated using a custom Taqman Copy Number
448 Assay (assay ID: cnvtaq1_CC1RVED; Applied Biosystems, Foster City, CA) for 94 birds
449 phenotyped by wing pigment pattern category and 89 birds whose pigmentation was
450 quantified by image analysis. After DNA extraction, samples were diluted to 5ng/μL.
451 Samples were run in quadruplicate according to the manufacturer's protocol.
452
453 **Quantification of pigment pattern phenotype**
454 At the time of blood sample collection, the right wing shield was photographed
455 (RAW format images from a Nikon D70 or Sony a6000 digital camera). In Photoshop
456 (Adobe Systems Incorporated, San Jose, CA), the wing shield including the bar (on the
457 secondary covert feathers) was isolated from the original RAW file. Images were
458 adjusted to remove shadows and the contrast was set to 100%. The isolated adjusted wing
459 shield image was then imported into ImageJ (imagej.nih.gov/) in JPEG format. Image
460 depth was set to 8-bit and we then applied the threshold command. Threshold was further
461 adjusted by hand to capture checkering and particles were analyzed using a minimum
462 pixel size of 50. This procedure calculated the area of dark plumage pigmentation on the
463 wing shield. Total shield area was calculated using the Huang threshold setting and

464 analyzing the particles as before (minimum pixel size of 50). The dark area particles were
465 divided by total wing area particles, and then multiplied by 100 to get the percent dark
466 area on the wing shield. Measurements were done in triplicate for each bird, and the
467 mean percentages of dark area for each bird were used to test for associations between
468 copy number and phenotype using a non-linear least squares regression.
469
470 **qRT-PCR analysis of gene expression**
471 Two secondary covert wing feathers each from the wing shields of 8 bar, 7
472 checker, and 8 T-check birds were plucked to stimulate feather regeneration for qRT-
473 PCR experiments. Nine days after plucking, regenerating feather buds were removed, the
474 proximal 5 mm was cut longitudinally, and specimens were stored in RNAlater (Qiagen,
475 Valencia, CA) at 4°C for up to three days. Next, collar cells were removed, RNA was
476 isolated, and mRNA was reverse-transcribed to cDNA as described previously (Domyan
477 et al. 2014). Intron-spanning primers (see Table S1) were used to amplify each target
478 using a CFX96 qPCR instrument and iTaq Universal Syber Green Supermix (Bio-Rad,
479 Hercules, CA). Samples were run in duplicate and normalized to β-actin. The mean value
480 was determined and results are presented as mean ± S.E. for each phenotype. Results
481 were compared using a Wilcoxon Rank Sum test and expression differences were
482 considered statistically-significant if $p < 0.05$.
483
484 **Allele-specific expression assay**
485 SNPs in *NDP* and *EFHC2* were identified as being diagnostic of the bar or
486 checker/T-check haplotypes from resequenced birds. Heterozygous birds were identified

by Sanger sequencing in the minimal checker haplotype region (AV17 primers, see Table S1). Twelve checker and T-check heterozygous birds were then verified by additional Sanger reactions (AV54 for *NDP* and AV97 for *EFHC2*, see Table S1) to be heterozygous for the SNPs in *NDP* and *EFHC2*. PyroMark Custom assays (Qiagen) were designed for each SNP using the manufacturer's software (Table S1). Pyrosequencing was performed on gDNA and cDNA derived from collar cells from 9-day regenerating feathers using a PyroMark Q24 instrument (Qiagen). Signal intensity ratios from the cDNA samples were normalized to the ratios from the corresponding gDNA samples to control for bias in allele amplification. Normalized ratios were analyzed by a Wilcoxon Rank Sum test and results were considered significant if $p < 0.05$.

NDP genotyping and alignments

NDP exons were sequenced using primers in Table S1. Primers pairs were designed using the rock pigeon reference genome (Cliv_1.0) (Shapiro et al. 2013). PCR products were purified using a QIAquick PCR purification kit (Qiagen) and Sanger sequenced. Sequences from each exon were then edited for quality with Sequencher v.5.1 (GeneCodes, Ann Arbor, MI). Sequences were translated and aligned with SIXFRAME and CLUSTALW in SDSC Biology Workbench (http://workbench.sdsc.edu). Amino acid sequences outside of Columbidae were downloaded from Ensembl (www.ensembl.org).

***D*-statistic calculations**

Whole genome ABBA-BABA (https://github.com/vcflib) was performed on 10 X 10 combinations of bar and checker (Table S2) birds in the arrangement: bar, checker, *C.*

510 *guinea*, *C. palumbus*. VCFLIB (https://github.com/vcflib) was used to smooth raw
511 ABBA-BABA results in 1000-kb or 100-kb windows for whole-genome or Scaffold 68
512 analyses respectively. For each 10 X 10 combination. We calculated the average D
513 statistic across the genome. These were then averaged to generate a whole genome
514 average of D=0.0212, marked as the dotted line in Fig. 4A. Confidence intervals were
515 generated via moving blocks bootstrap (Kunsch 1989). Block sizes are equal to the
516 windows above, with D-statistic values resampled with replacement a number of times
517 equal to the number of windows in a sample. In Figure 4A, three representative ABBA-
518 BABA tests are shown for different combinations of bar and checker birds. The checker
519 and bar birds used in each representative comparison are: ARC-STA, SRS346901 and
520 SRS346887; MAP-ORR, SRS346893 and SRS346881; IRT-STA, SRS346892 and
521 SRS346887 respectively.
522
523 **Haplotype phasing and HybridCheck analysis**
524 VCF files containing Scaffold 68 genotypes for 16 bar, 11 homozygous checker,
525 and 1 *C. guinea* were phased using Beagle version 3.3 (Browning and Browning 2007).
526 VCFs were then converted to fasta format using vcf2fasta in vcf-lib
527 (https://github.com/vcflib). HybridCheck (Ward and van Oosterhout 2016)
528 (https://github.com/Ward9250/HybridCheck) was run to visualize pairwise sequence
529 similarities between trios of bar, checker, and *C. guinea* sequences across Scaffold 68.
530
531 **Pairwise SNP comparisons**

Phased VCF files for 16 bar, 11 homozygous checker, and 1 *C. guinea* were subsetted to the minimal checker haplotype region (positions 1,702,691-1,805,600) with tabix (Li 2011). The vcf-compare software module (VCFtools, Danecek et al. 2011) was used to run pairwise comparisons between bar, checker, and *C. guinea* birds (176 bar-checker, 16 bar-guinea, and 11 checker-guinea comparisons) as well as among bar and checker birds (120 bar-bar and 55 checker-checker comparisons). The total number of differences for each group was compared to the number of differences that are expected to accumulate during a 4-5 million year divergence time in a 102,909-bp region (the size of the minimal checker haplotype) with the mutation rate μ=1.42e-9 (Shapiro et al. 2013) using the coalescent equation: Time= #SNPs/(2xμx length of the region). The observed pairwise differences and the expected number of differences were evaluated with two-sample t-tests and all groups were considered statistically different from the 4-5 MY expectation (1169.05-1461.31). Standard deviations from the mean number of differences for each group were calculated in R: bar-*guinea*, 109; bar-checker, 99; bar-bar, 143; checker-*guinea*, 6; checker-checker, 8.

Transcript amplification of barless allele of *NDP*

In order to determine whether the barless allele of *NDP* is transcribed and persists in the cell, or is degraded by the non-sense mediated decay (NMD) pathway, we designed a PCR assay to amplify *NDP* mRNA using intron-spanning primers (see Table S1). 4 barless, 2 bar, 2 checker, and 2 T-check birds were plucked to stimulate regeneration for NDP amplification. Feathers were harvested, RNA extracted, and cDNA synthesized as above. We detected expression of *NDP* in feather buds from barless feathers (n=4

555 feathers from a single individual). While not quantitative, expression was qualitatively
556 similar to the levels of amplicons generated from other pattern phenotypes (n=2 for bar,
557 checker, and T-check).
558
559 ***EFHC2* alignments**
560 *EFHC2* exonic sequences from resequenced homozygous bar (n=16),
561 homozygous check or T-check (n=11), barless (n=9), *Columba rupestris* (n=1), *Columba*
562 *guinea* (n=1), and *Columba palumbus* (n=1) were extracted using the IGV browser
563 (Thorvaldsdottir et al. 2013). Exon sequences for each group were translated using
564 SIXFRAME in SDSC Biology Workbench (http://workbench.sdsc.edu). Peptide
565 sequences were then aligned to EFHC2 amino acid sequences from other species
566 downloaded from ensembl (http://www.ensembl.org) using CLUSTALW (Thompson et
567 al. 1994) in SDSC Biology Workbench. Exon sequences from additional *C. livia* (n=17
568 checker or T-check and n=14 bar) and *C. guinea* (n=5) birds were determined by Sanger
569 sequencing.
570
571 **Recombination rate estimation**
572 Recombination frequency estimates were generated from a genetic map based an
573 F2 cross of two divergent *C. livia* breeds, a Pomeranian Pouter and a Scandaroon
574 (Domyan et al. 2016). Briefly, for genetic map construction, genotyping by sequencing
575 (GBS) data were generated, trimmed, and filtered as described (Domyan et al. 2016),
576 then mapped to the pigeon Cliv_1.0 pigeon genome assembly using Bowtie2 (Langmead
577 and Salzberg 2012). Genotypes were called using Stacks (Catchen et al. 2011), and

genetic map construction was performed using R/qtl (www.rqtl.org) (Broman et al. 2003). Pairwise recombination frequencies were calculated for all markers based on GBS genotypes. Within individual scaffolds, markers were filtered to remove loci showing segregation distortion (Chi-square, $p < 0.01$) or probable genotyping error. Specifically, markers were removed if dropping the marker led to an increased LOD score, or if removing a non-terminal marker led to a decrease in length of >10 cM that was not supported by physical distance. Individual genotypes with error LOD scores >5 (Lincoln and Lander 1992) were also removed. Pairwise recombination frequencies for markers retained in the final linkage map were used to estimate the age of the introgression event between *C. guinea* and *C. livia.*

Minimal haplotype age estimation

The minimal haplotype age was estimated following Voight et al. (2006). We assume a star-shaped phylogeny, in which all samples with the minimal haplotype are identical to the nearest recombination event, and differ immediately beyond it. Choosing a variant in the center of the minimal haplotype, we calculated EHH, and estimated the age using the largest haplotype with a probability of homozygosity just below 0.25. Note that

$$\Pr[homoz] = e^{-2rg}$$

where r is the genetic map distance, and g is the number of generations since introgression / onset of selection. Therefore

$$g = -\frac{100 \log(\Pr[homoz])}{2r}$$

The confidence interval around g was estimated assuming

$$N \sim Binom(n = 22, p = 0.204)$$

Here, N is a binomially distributed random variable for the number of samples that have not recombined to a map distance equal to 2r. Then, Pr[homoz] = N / 22. The probability that a sample has no recombination event within 2r of the focal SNP is p = (Pr[homoz | left] + Pr[homoz | right]) / 2 is derived from the data. Both left and right of the focal SNP we chose the end of the haplotype at the first SNP which brought Pr[homoz] < 0.25.

ACKNOWLEDGEMENTS

We thank past and present members of the Shapiro lab for assistance with sample collection and processing; members of the Utah Pigeon Club and National Pigeon Association for sample contributions; and Gene Hochlan, Gary Young, and Robert Mangile for critical discussions and advice. Mr. Hochlan also generously provided feather samples from *C. guinea* that helped us assess feasibility of the introgression study. We thank Fred Adler, Brett Boyd, Elena Boer, Robert Greenhalgh, J.J. Horns, Christopher Leonard, Raquel Maynez, Jon Seger, and Scott Villa for technical assistance and advice. Dale Clayton and Sarah Bush generously provided field-collected tissue samples of *C. guinea* and *C. palumbus* for whole-genome sequencing. We thank Safari West (Santa Rosa, CA), the Louisiana State University Museum of Natural Science, nad the University of Washington Burke Museum for additional *C. guinea* tissue samples (museum accessions 95045 JK 00 179, 101559 BCA 523, and 119004 EEM 979). This work was supported by the National Science Foundation (CAREER DEB-1149160 to M.D.S.; GRF 1256065 to A.I.V. and R.B.; and DEB-1342604 to K.P.J.) and the National

624 Institutes of Health (R01GM115996 to M.D.S., R01GM104390 to M.Y.; fellowships
625 T32GM007464 to Z.K. and R25CA057730 to R.J.B.). E.T.M. is a fellow of the Jane
626 Coffin Childs Memorial Fund for Medical Research. The funders had no role in study
627 design, data collection and analysis, decision to publish, or preparation of the manuscript.
628 We acknowledge a computer time allocation from the Center for High Performance
629 Computing at the University of Utah.

630

631 **Author contributions:** A.I.V., Z.K., C.D.H., M.Y., and M.D.S. designed research;
632 A.I.V., Z.K., R.B., and E.M. performed research; A.I.V., Z.K., R.B., E.M., R.J.M.,
633 E.T.M., E.J.O., and M.D.S. analyzed data; K.P.J. contributed biological samples and
634 genome sequence data; and A.I.V. and M.D.S. wrote the paper with input from the other
635 authors.

636

637 **LITERATURE CITED**

638 Adzhubei, I. A., S. Schmidt, L. Peshkin, V. E. Ramensky, A. Gerasimova, P. Bork, A. S.
639 Kondrashov, and S. R. Sunyaev. 2010. A method and server for predicting
640 damaging missense mutations. Nat Methods 7:248-249.
641 Allen, R. C., S. R. Russell, L. M. Streb, A. Alsheikheh, and E. M. Stone. 2006.
642 Phenotypic heterogeneity associated with a novel mutation (Gly112Glu) in the
643 Norrie disease protein. Eye 20:234-241.
644 Anderson, T. M., B. M. vonHoldt, S. I. Candille, M. Musiani, C. Greco, D. R. Stahler, D.
645 W. Smith, B. Padhukasahasram, E. Randi, J. A. Leonard, C. D. Bustamante, E. A.
646 Ostrander, H. Tang, R. K. Wayne, and G. S. Barsh. 2009. Molecular and
647 evolutionary history of melanism in North American gray wolves. Science
648 323:1339-1343.
649 Berger, W. 1998. Molecular dissection of Norrie disease. Acta anatomica 162:95-100.
650 Blaya, C., P. Moorjani, G. A. Salum, L. Goncalves, L. A. Weiss, S. Leistner-Segal, G. G.
651 Manfro, and J. W. Smoller. 2009. Preliminary evidence of association between
652 EFHC2, a gene implicated in fear recognition, and harm avoidance. Neuroscience
653 letters 452:84-86.
654 Bonhote, J. L. and F. W. Smalley. 1911. On Colour and Colour-pattern Inheritance in
655 Pigeons. Proceedings of the Zoological Society of London 81:601-628.
656 Broman, K., H. Wu, S. Sen, and G. Churchill. 2003. R/qtl: QTL mapping in experimental
657 crosses. Bioinformatics 19:889-890.
658 Browning, S. R. and B. L. Browning. 2007. Rapid and accurate haplotype phasing and
659 missing-data inference for whole-genome association studies by use of localized
660 haplotype clustering. Am J Hum Genet 81:1084-1097.
661 Burley, N. 1981. Mate Choice by Multiple Criteria in a Monogamous Species. American
662 Naturalist 117:515-528.
663 Čanády, A. and L. Mošanský. 2013. Population size and plumage polymorphism of feral
664 pigeon (Columba liviaformaurbana) from urban environment of Košice city
665 (Slovakia). Zoology and Ecology 23:104-110.
666 Catchen, J. M., A. Amores, P. Hohenlohe, W. Cresko, and J. H. Postlethwait. 2011.
667 Stacks: building and genotyping loci de novo from short-read sequences. G3
668 1:171-182.
669 Chan, Y. F., M. E. Marks, F. C. Jones, G. Villarreal, Jr., M. D. Shapiro, S. D. Brady, A.
670 M. Southwick, D. M. Absher, J. Grimwood, J. Schmutz, R. M. Myers, D. Petrov,
671 B. Jonsson, D. Schluter, M. A. Bell, and D. M. Kingsley. 2010. Adaptive
672 evolution of pelvic reduction in sticklebacks by recurrent deletion of a *Pitx1*
673 enhancer. Science 327:302-305.
674 Chatelain, M., J. Gasparini, and A. Frantz. 2016. Do trace metals select for darker birds
675 in urban areas? An experimental exposure to lead and zinc. Global Change
676 Biology 22:2380–2391.
677 Chatelain, M., J. Gasparini, L. Jacquin, and A. Frantz. 2014. The adaptive function of
678 melanin-based plumage coloration to trace metals. Biol Lett 10:20140164.
679 Chen, Z. Y., R. W. Hendriks, M. A. Jobling, J. F. Powell, X. O. Breakefield, K. B. Sims,
680 and I. W. Craig. 1992. Isolation and characterization of a candidate gene for
681 Norrie disease. Nat Genet 1:204-208.

682 Coulson, T., D. R. MacNulty, D. R. Stahler, B. vonHoldt, R. K. Wayne, and D. W.
683 Smith. 2011. Modeling effects of environmental change on wolf population
684 dynamics, trait evolution, and life history. Science 334:1275-1278.
685 Danecek, P., A. Auton, G. Abecasis, C. A. Albers, E. Banks, M. A. DePristo, R. E.
686 Handsaker, G. Lunter, G. T. Marth, S. T. Sherry, G. McVean, and R. Durbin.
687 2011. The variant call format and VCFtools. Bioinformatics 27:2156-2158.
688 Darwin, C. 1859. On the Origin of Species by Means of Natural Selection. John Murray,
689 London.
690 Darwin, C. 1868. The Variation of Plants and Animals under Domestication. John
691 Murray, London.
692 del Hoyo, J., A. Elliott, J. Sargatal, D. A. Christie, and E. de Juana, eds. 2017. Handbook
693 of the Birds of the World Alive (http://www.hbw.com/). Lynx Edicions,
694 Barcelona.
695 Deng, C., P. Reddy, Y. Cheng, C. W. Luo, C. L. Hsiao, and A. J. Hsueh. 2013. Multi-
696 functional norrin is a ligand for the LGR4 receptor. Journal of cell science
697 126:2060-2068.
698 Domyan, E. T., M. W. Guernsey, Z. Kronenberg, S. Krishnan, R. E. Boissy, A. I.
699 Vickrey, C. Rodgers, P. Cassidy, S. A. Leachman, J. W. Fondon, 3rd, M. Yandell,
700 and M. D. Shapiro. 2014. Epistatic and combinatorial effects of pigmentary gene
701 mutations in the domestic pigeon. Curr Biol 24:459-464.
702 Domyan, E. T., Z. Kronenberg, C. R. Infante, A. I. Vickrey, S. A. Stringham, R. Bruders,
703 M. W. Guernsey, S. Park, J. Payne, R. B. Beckstead, G. Kardon, D. B. Menke, M.
704 Yandell, and M. D. Shapiro. 2016. Molecular shifts in limb identity underlie
705 development of feathered feet in two domestic avian species. eLife 5:e12115.
706 Domyan, E. T. and M. D. Shapiro. 2017. Pigeonetics takes flight: Evolution,
707 development, and genetics of intraspecific variation. Dev Biol 427:241-250.
708 Durand, E. Y., N. Patterson, D. Reich, and M. Slatkin. 2011. Testing for ancient
709 admixture between closely related populations. Mol Biol Evol 28:2239-2252.
710 Eom, D. S., E. J. Bain, L. B. Patterson, M. E. Grout, and D. M. Parichy. 2015. Long-
711 distance communication by specialized cellular projections during pigment
712 pattern development and evolution. Elife 4.
713 Eriksson, J., G. Larson, U. Gunnarsson, B. Bed'hom, M. Tixier-Boichard, L. Stromstedt,
714 D. Wright, A. Jungerius, A. Vereijken, E. Randi, P. Jensen, and L. Andersson.
715 2008. Identification of the yellow skin gene reveals a hybrid origin of the
716 domestic chicken. PLoS Genet 4:e1000010.
717 Gierasch, L. M. 1989. Signal sequences. Biochemistry 28:923-930.
718 Harrison, R. G. and E. L. Larson. 2014. Hybridization, introgression, and the nature of
719 species boundaries. J Hered 105 Suppl 1:795-809.
720 Hedrick, P. W. 2013. Adaptive introgression in animals: examples and comparison to
721 new mutation and standing variation as sources of adaptive variation. Mol Ecol
722 22:4606-4618.
723 Hendrickx, M. and L. Leyns. 2008. Non-conventional Frizzled ligands and Wnt
724 receptors. Development, growth & differentiation 50:229-243.
725 Hill, G. E. and K. J. McGraw, eds. 2006. Bird Coloration, Volume 2: Function and
726 Evolution. Harvard University Press.

727 Hollander, W. F. 1937. Hereditary Interrelationships of Certain Factors in Pigeons. Pp.
728 67. Department of Genetics. University of Wisconsin.
729 Hollander, W. F. 1938. Inheritance of certain "blue-black" patterns and "bleached"
730 colorations in the domestic pigeon. Genetics 23:12-23.
731 Hollander, W. F. 1983. Origins and Excursions in Pigeon Genetics. The Ink Spot, Burton,
732 Kansas.
733 Hollander, W. F. and W. J. Miller. 1981. Hereditary variants of behavior and vision in the
734 pigeon. Iowa State Journal of Research 55:323-331.
735 Holmes, L. B. 1971. Norrie's disease: An X-linked syndrome of retinal malformation,
736 mental retardation, and deafness. J Pediatrics 79:89-92.
737 Holt, C., M. Campbell, D. A. Keays, N. Edelman, A. Kapusta, E. Maclary, E. Domyan,
738 A. Suh, W. C. Warren, M. Yandell, M. T. P. Gilbert, and M. D. Shapiro. 2017.
739 Improved genome assembly and annotation for the rock pigeon (*Columba livia*).
740 bioRxiv:doi: https://doi.org/10.1101/220947.
741 Hubbard, J. K., J. A. Uy, M. E. Hauber, H. E. Hoekstra, and R. J. Safran. 2010.
742 Vertebrate pigmentation: from underlying genes to adaptive function. Trends
743 Genet 26:231-239.
744 Huerta-Sanchez, E., X. Jin, Asan, Z. Bianba, B. M. Peter, N. Vinckenbosch, Y. Liang, X.
745 Yi, M. He, M. Somel, P. Ni, B. Wang, X. Ou, Huasang, J. Luosang, Z. X. Cuo, K.
746 Li, G. Gao, Y. Yin, W. Wang, X. Zhang, X. Xu, H. Yang, Y. Li, J. Wang, J.
747 Wang, and R. Nielsen. 2014. Altitude adaptation in Tibetans caused by
748 introgression of Denisovan-like DNA. Nature 512:194-197.
749 Irwin, M. R., L. J. Cole, and C. D. Gordo. 1936. Immunogenetic studies of species and
750 species hybrids in pigeons, and the separation of species-specific characters in
751 backcross generations. J Exp Zool 73:285-308.
752 Isashiki, Y., N. Ohba, T. Yanagita, N. Hokita, N. Doi, M. Nakagawa, M. Ozawa, and N.
753 Kuroda. 1995. Novel mutation at the initiation codon in the Norrie disease gene in
754 two Japanese families. Human Genetics 95:105-108.
755 Jacquin, L., C. Recapet, P. Bouche, G. Leboucher, and J. Gasparini. 2012. Melanin-based
756 coloration reflects alternative strategies to cope with food limitation in pigeons.
757 Behavioral Ecology 23:907-915.
758 Johnston, R. F. and M. Janiga. 1995. Feral Pigeons. Oxford University Press.
759 Johnston, R. F. and S. Johnson. 1989. Nonrandom mating in feral pigeons. Condor 91:23-
760 29.
761 Jones, S. v. H. 1922. Studies on inheritance in pigeons. IV. Checks and bars and other
762 modificaitons of black. Genetics 7:466-507.
763 Kaelin, C. B., X. Xu, L. Z. Hong, V. A. David, K. A. McGowan, A. Schmidt-Kuntzel, M.
764 E. Roelke, J. Pino, J. Pontius, G. M. Cooper, H. Manuel, W. F. Swanson, L.
765 Marker, C. K. Harper, A. van Dyk, B. Yue, J. C. Mullikin, W. C. Warren, E.
766 Eizirik, L. Kos, S. J. O'Brien, G. S. Barsh, and M. Menotti-Raymond. 2012.
767 Specifying and sustaining pigmentation patterns in domestic and wild cats.
768 Science 337:1536-1541.
769 Kaloglu, C., I. Cesur, and H. E. Bulut. 2011. Norrin immunolocalization and its possible
770 functions in rat endometrium during the estrus cycle and early pregnancy.
771 Development, growth & differentiation 53:887-896.

Karczewska-Kupczewska, M., M. Stefanowicz, N. Matulewicz, A. Nikolajuk, and M. Straczkowski. 2016. Wnt Signaling Genes in Adipose Tissue and Skeletal Muscle of Humans With Different Degrees of Insulin Sensitivity. The Journal of clinical endocrinology and metabolism 101:3079-3087.

Ke, J., K. G. Harikumar, C. Erice, C. Chen, X. Gu, L. Wang, N. Parker, Z. Cheng, W. Xu, B. O. Williams, K. Melcher, L. J. Miller, and H. E. Xu. 2013. Structure and function of Norrin in assembly and activation of a Frizzled 4-Lrp5/6 complex. Genes Dev 27:2305-2319.

Kelsh, R. N. 2004. Genetics and evolution of pigment patterns in fish. Pigment Cell Res 17:326-336.

Kelsh, R. N., M. L. Harris, S. Colanesi, and C. A. Erickson. 2009. Stripes and belly-spots -- a review of pigment cell morphogenesis in vertebrates. Semin Cell Dev Biol 20:90-104.

Kronenberg, Z. N., E. J. Osborne, K. R. Cone, B. J. Kennedy, E. T. Domyan, M. D. Shapiro, N. C. Elde, and M. Yandell. 2015. Wham: Identifying Structural Variants of Biological Consequence. PLoS Comput Biol 11:e1004572.

Kunsch, H. R. 1989. The Jackknife and the Bootstrap for General Stationary Observations. Annals of Statistics 17:1217-1241.

Lamichhaney, S., J. Berglund, M. S. Almen, K. Maqbool, M. Grabherr, A. Martinez-Barrio, M. Promerova, C. J. Rubin, C. Wang, N. Zamani, B. R. Grant, P. R. Grant, M. T. Webster, and L. Andersson. 2015. Evolution of Darwin's finches and their beaks revealed by genome sequencing. Nature 518:371-375.

Langmead, B. and S. L. Salzberg. 2012. Fast gapped-read alignment with Bowtie 2. Nat Methods 9:357-359.

Levi, W. M. 1986. The Pigeon (Second Revised Edition). Levi Publishing Co., Inc., Sumter, S.C.

Li, H. 2011. Tabix: fast retrieval of sequence features from generic TAB-delimited files. Bioinformatics 27:718-719.

Lin, C. M., T. X. Jiang, R. E. Baker, P. K. Maini, R. B. Widelitz, and C. M. Chuong. 2009. Spots and stripes: pleomorphic patterning of stem cells via p-ERK-dependent cell chemotaxis shown by feather morphogenesis and mathematical simulation. Dev Biol 334:369-382.

Lin, S. J., J. Foley, T. X. Jiang, C. Y. Yeh, P. Wu, A. Foley, C. M. Yen, Y. C. Huang, H. C. Cheng, C. F. Chen, B. Reeder, S. H. Jee, R. B. Widelitz, and C. M. Chuong. 2013. Topology of feather melanocyte progenitor niche allows complex pigment patterns to emerge. Science 340:1442-1445.

Linck, R., X. Fu, J. Lin, C. Ouch, A. Schefter, W. Steffen, P. Warren, and D. Nicastro. 2014. Insights into the structure and function of ciliary and flagellar doublet microtubules: tektins, Ca2+-binding proteins, and stable protofilaments. J Biol Chem 289:17427-17444.

Lincoln, S. E. and E. S. Lander. 1992. Systematic detection of errors in genetic linkage data. Genomics 14:604-610.

Linnen, C. R., Y. P. Poh, B. K. Peterson, R. D. Barrett, J. G. Larson, J. D. Jensen, and H. E. Hoekstra. 2013. Adaptive evolution of multiple traits through multiple mutations at a single gene. Science 339:1312-1316.

817 Liu, K. J., E. Steinberg, A. Yozzo, Y. Song, M. H. Kohn, and L. Nakhleh. 2015.
818 Interspecific introgressive origin of genomic diversity in the house mouse. Proc
819 Natl Acad Sci U S A 112:196-201.
820 Lofts, B., R. K. Murton, and N. J. Westwood. 1966. Gonadal cycles and the evolution of
821 breeding seasons in British Columbidae. Journal of Zoology, London 150:249-
822 272.
823 Loh, N. Y., M. J. Neville, K. Marinou, S. A. Hardcastle, B. A. Fielding, E. L. Duncan, M.
824 I. McCarthy, J. H. Tobias, C. L. Gregson, F. Karpe, and C. Christodoulides. 2015.
825 LRP5 regulates human body fat distribution by modulating adipose progenitor
826 biology in a dose- and depot-specific fashion. Cell metabolism 21:262-272.
827 Lopes, R. J., J. D. Johnson, M. B. Toomey, M. S. Ferreira, P. M. Araujo, J. Melo-
828 Ferreira, L. Andersson, G. E. Hill, J. C. Corbo, and M. Carneiro. 2016. Genetic
829 Basis for Red Coloration in Birds. Curr Biol 26:1427-1434.
830 Luhmann, U. F., D. Meunier, W. Shi, A. Luttges, C. Pfarrer, R. Fundele, and W. Berger.
831 2005. Fetal loss in homozygous mutant Norrie disease mice: a new role of Norrin
832 in reproduction. Genesis 42:253-262.
833 MacManes, M. D., S. H. Austin, A. S. Lang, A. Booth, V. Farrar, and R. M. Calisi. 2017.
834 Widespread patterns of sexually dimorphic gene expression in an avian
835 hypothalamic-pituitary-gonadal (HPG) axis. Scientific reports 7:45125.
836 Mallarino, R., C. Henegar, M. Mirasierra, M. Manceau, C. Schradin, M. Vallejo, S.
837 Beronja, G. S. Barsh, and H. E. Hoekstra. 2016. Developmental mechanisms of
838 stripe patterns in rodents. Nature 539:518-523.
839 Manceau, M., V. S. Domingues, C. R. Linnen, E. B. Rosenblum, and H. E. Hoekstra.
840 2010. Convergence in pigmentation at multiple levels: mutations, genes and
841 function. Philosophical transactions of the Royal Society of London. Series B,
842 Biological sciences 365:2439-2450.
843 Mangile, R. J. 1987. What is "foggy" vision? American Pigeon Journal:27-28.
844 McGregor, A. P., V. Orgogozo, I. Delon, J. Zanet, D. G. Srinivasan, F. Payre, and D. L.
845 Stern. 2007. Morphological evolution through multiple cis-regulatory mutations at
846 a single gene. Nature 448:587-590.
847 Meindl, A., B. Lorenz, H. Achatz, H. Hellebrand, P. Schmitz-Valckenberg, and T.
848 Meitinger. 1995. Missense mutations in the NDP gene in patients with a less
849 severe course of Norrie disease. Hum Mol Genet 4:489-490.
850 Miller, C. T., S. Beleza, A. A. Pollen, D. Schluter, R. A. Kittles, M. D. Shriver, and D.
851 M. Kingsley. 2007. cis-Regulatory Changes in Kit Ligand Expression and Parallel
852 Evolution of Pigmentation in Sticklebacks and Humans. Cell 131:1179-1189.
853 Miller, W. J. 1953. The Time of Appearance of Species-Specific Antigens of *Columba*
854 *guinea* in the Embryos of Backcross Hybrids. Physiological Zoology 26:124-131.
855 Murton, R. K., N. J. Westwood, and R. J. P. Thearle. 1973. Polymorphism and the
856 evolution of a continuous breeding season in the pigeon, *Columba livia*. Journal
857 of Reproduction and Fertility. Supplement. 19:563-577.
858 Norrie, G. 1927. Causes of blindness in children. Acta Ophthalmil 5:357-386.
859 O'Brown, N. M., B. R. Summers, F. C. Jones, S. D. Brady, and D. M. Kingsley. 2015. A
860 recurrent regulatory change underlying altered expression and Wnt response of
861 the stickleback armor plates gene EDA. Elife 4:e05290.

862 Obukhova, N. Y. and A. G. Kreslavskii. 1984. Izmenchivost' i nasledovanie okraski u
863 sizykh golubei. Zool Zhurnal 64:1685-1694.
864 Ohlmann, A., R. Merkl, and E. R. Tamm. 2012. Focus on molecules: Norrin.
865 Experimental eye research 102:109-110.
866 Ohlmann, A. and E. R. Tamm. 2012. Norrin: molecular and functional properties of an
867 angiogenic and neuroprotective growth factor. Progress in retinal and eye research
868 31:243-257.
869 Paxton, C. N., S. B. Bleyl, S. C. Chapman, and G. C. Schoenwolf. 2010. Identification of
870 differentially expressed genes in early inner ear development. Gene expression
871 patterns : GEP 10:31-43.
872 Pejaver, V., J. Urresti, J. Lugo-Martinez, K. A. Pagel, G. N. Lin, H.-J. Nam, M. Mort, D.
873 N. Cooper, J. Sebat, L. M. Iakoucheva, S. D. Mooney, and P. Radivojac. 2017.
874 MutPred2: inferring the molecular and phenotypic impact of amino acid variants.
875 bioRxiv.
876 Petersen, N. and K. Williamson. 1949a. Polymorphism and breeding of the rock dove in
877 the Faroe Islands. Ibis 91:17-23.
878 Petersen, N. F. and K. Williamson. 1949b. Polymorphism and breeding of the rock dove
879 in the Faeroe Islands. Ibis 91:17-23.
880 Podhradsky, V. 1968. Influence of some exongenous factors on the pigmentation of some
881 domesticated pigeon phenotypes. Biológia 23:113-123.
882 Poelstra, J. W., N. Vijay, M. P. Hoeppner, and J. B. Wolf. 2015. Transcriptomics of
883 colour patterning and coloration shifts in crows. Mol Ecol 24:4617-4628.
884 Protas, M. E. and N. H. Patel. 2008. Evolution of coloration patterns. Annual review of
885 cell and developmental biology 24:425-446.
886 Rieseberg, L. 2011. Adaptive introgression: the seeds of resistance. Curr Biol 21:R581-
887 583.
888 Rosenblum, E. B., C. E. Parent, and E. E. Brandt. 2014. The Molecular Basis of
889 Phenotypic Convergence. Annual Review of Ecology, Evolution, and Systematics
890 45:203-226.
891 Roulin, A. and A. L. Ducrest. 2013. Genetics of colouration in birds. Semin Cell Dev
892 Biol 24:594-608.
893 Sabeti, P. C., P. Varilly, B. Fry, J. Lohmueller, E. Hostetter, C. Cotsapas, X. Xie, E. H.
894 Byrne, S. A. McCarroll, R. Gaudet, S. F. Schaffner, E. S. Lander, K. A. Frazer, D.
895 G. Ballinger, D. R. Cox, D. A. Hinds, L. L. Stuve, R. A. Gibbs, J. W. Belmont, A.
896 Boudreau, P. Hardenbol, S. M. Leal, S. Pasternak, D. A. Wheeler, T. D. Willis, F.
897 Yu, H. Yang, C. Zeng, Y. Gao, H. Hu, W. Hu, C. Li, W. Lin, S. Liu, H. Pan, X.
898 Tang, J. Wang, W. Wang, J. Yu, B. Zhang, Q. Zhang, H. Zhao, J. Zhou, S. B.
899 Gabriel, R. Barry, B. Blumenstiel, A. Camargo, M. Defelice, M. Faggart, M.
900 Goyette, S. Gupta, J. Moore, H. Nguyen, R. C. Onofrio, M. Parkin, J. Roy, E.
901 Stahl, E. Winchester, L. Ziaugra, D. Altshuler, Y. Shen, Z. Yao, W. Huang, X.
902 Chu, Y. He, L. Jin, Y. Liu, W. Sun, H. Wang, Y. Wang, X. Xiong, L. Xu, M. M.
903 Waye, S. K. Tsui, H. Xue, J. T. Wong, L. M. Galver, J. B. Fan, K. Gunderson, S.
904 S. Murray, A. R. Oliphant, M. S. Chee, A. Montpetit, F. Chagnon, V. Ferretti, M.
905 Leboeuf, J. F. Olivier, M. S. Phillips, S. Roumy, C. Sallee, A. Verner, T. J.
906 Hudson, P. Y. Kwok, D. Cai, D. C. Koboldt, R. D. Miller, L. Pawlikowska, P.
907 Taillon-Miller, M. Xiao, L. C. Tsui, W. Mak, Y. Q. Song, P. K. Tam, Y.

908 Nakamura, T. Kawaguchi, T. Kitamoto, T. Morizono, A. Nagashima, Y. Ohnishi,
909 A. Sekine, T. Tanaka, T. Tsunoda, P. Deloukas, C. P. Bird, M. Delgado, E. T.
910 Dermitzakis, R. Gwilliam, S. Hunt, J. Morrison, D. Powell, B. E. Stranger, P.
911 Whittaker, D. R. Bentley, M. J. Daly, P. I. de Bakker, J. Barrett, Y. R. Chretien, J.
912 Maller, S. McCarroll, N. Patterson, I. Pe'er, A. Price, S. Purcell, D. J. Richter, P.
913 Sabeti, R. Saxena, P. C. Sham, L. D. Stein, L. Krishnan, A. V. Smith, M. K.
914 Tello-Ruiz, G. A. Thorisson, A. Chakravarti, P. E. Chen, D. J. Cutler, C. S.
915 Kashuk, S. Lin, G. R. Abecasis, W. Guan, Y. Li, H. M. Munro, Z. S. Qin, D. J.
916 Thomas, G. McVean, A. Auton, L. Bottolo, N. Cardin, S. Eyheramendy, C.
917 Freeman, J. Marchini, S. Myers, C. Spencer, M. Stephens, P. Donnelly, L. R.
918 Cardon, G. Clarke, D. M. Evans, A. P. Morris, B. S. Weir, T. A. Johnson, J. C.
919 Mullikin, S. T. Sherry, M. Feolo, A. Skol, H. Zhang, I. Matsuda, Y. Fukushima,
920 D. R. Macer, E. Suda, C. N. Rotimi, C. A. Adebamowo, I. Ajayi, T. Aniagwu, P.
921 A. Marshall, C. Nkwodimmah, C. D. Royal, M. F. Leppert, M. Dixon, A. Peiffer,
922 R. Qiu, A. Kent, K. Kato, N. Niikawa, I. F. Adewole, B. M. Knoppers, M. W.
923 Foster, E. W. Clayton, J. Watkin, D. Muzny, L. Nazareth, E. Sodergren, G. M.
924 Weinstock, I. Yakub, B. W. Birren, R. K. Wilson, L. L. Fulton, J. Rogers, J.
925 Burton, N. P. Carter, C. M. Clee, M. Griffiths, M. C. Jones, K. McLay, R. W.
926 Plumb, M. T. Ross, S. K. Sims, D. L. Willey, Z. Chen, H. Han, L. Kang, M.
927 Godbout, J. C. Wallenburg, P. L'Archeveque, G. Bellemare, K. Saeki, D. An, H.
928 Fu, Q. Li, Z. Wang, R. Wang, A. L. Holden, L. D. Brooks, J. E. McEwen, M. S.
929 Guyer, V. O. Wang, J. L. Peterson, M. Shi, J. Spiegel, L. M. Sung, L. F. Zacharia,
930 F. S. Collins, K. Kennedy, R. Jamieson and J. Stewart. 2007. Genome-wide
931 detection and characterization of positive selection in human populations. Nature
932 449:913-918.
933 Sell, A. 2012. Pigeon Genetics: Applied Genetics in the Domestic Pigeon. Verlag Karin
934 und A. Sell, Achim, Germany.
935 Shapiro, M. D. and E. T. Domyan. 2013. Domestic pigeons. Curr Biol 23:R302-303.
936 Shapiro, M. D., Z. Kronenberg, C. Li, E. T. Domyan, H. Pan, M. Campbell, H. Tan, C. D.
937 Huff, H. Hu, A. I. Vickrey, S. C. Nielsen, S. A. Stringham, H. Hu, E. Willerslev,
938 M. T. Gilbert, M. Yandell, G. Zhang, and J. Wang. 2013. Genomic diversity and
939 evolution of the head crest in the rock pigeon. Science 339:1063-1067.
940 Shapiro, M. D., M. E. Marks, C. L. Peichel, B. K. Blackman, K. S. Nereng, B. Jonsson,
941 D. Schluter, and D. M. Kingsley. 2004. Genetic and developmental basis of
942 evolutionary pelvic reduction in threespine sticklebacks. Nature 428:717-723.
943 Sims, K. B., R. V. Lebo, G. Benson, C. Shalish, D. Schuback, Z. Y. Chen, G. Bruns, I.
944 W. Craig, M. S. Golbus, and X. O. Breakefield. 1992. The Norrie disease gene
945 maps to a 150 kb region on chromosome Xp11.3. Hum Mol Genet 1:83-89.
946 Smallwood, P. M., J. Williams, Q. Xu, D. J. Leahy, and J. Nathans. 2007. Mutational
947 analysis of Norrin-Frizzled4 recognition. J Biol Chem 282:4057-4068.
948 Song, Y., S. Endepols, N. Klemann, D. Richter, F. R. Matuschka, C. H. Shih, M. W.
949 Nachman, and M. H. Kohn. 2011. Adaptive introgression of anticoagulant rodent
950 poison resistance by hybridization between old world mice. Curr Biol 21:1296-
951 1301.

952 Startin, C. M., C. Fiorentini, M. de Haan, and D. H. Skuse. 2015. Variation in the X-
953 linked EFHC2 gene is associated with social cognitive abilities in males. PLoS
954 One 10:e0131604.
955 Stringham, S. A., E. A. Mulroy, J. Xing, D. Record, M. W. Guernsey, J. T. Aldenhoven,
956 E. J. Osborne, and M. D. Shapiro. 2012. Divergence, convergence, and the
957 ancestry of feral populations in the domestic rock pigeon. Curr Biol 22:302-308.
958 Taibel, A. M. 1949. Nuovi risultati d'incrocio diretto e reciproco fra <<*Columba livia*
959 *domestica*>> e <<*Columba guinea*>>. Archivio Zoologico Italiano 34:431-476.
960 Thompson, J. D., D. G. Higgins, and T. J. Gibson. 1994. CLUSTAL W: improving the
961 sensitivity of progressive multiple sequence alignment through sequence
962 weighting, position-specific gap penalties and weight matrix choice. Nucleic
963 Acids Res 22:4673-4680.
964 Thorvaldsdottir, H., J. T. Robinson, and J. P. Mesirov. 2013. Integrative Genomics
965 Viewer (IGV): high-performance genomics data visualization and exploration.
966 Briefings in bioinformatics 14:178-192.
967 Voight, B. F., S. Kudaravalli, X. Wen, and J. K. Pritchard. 2006. A map of recent positive
968 selection in the human genome. PLoS Biol 4:e72.
969 Warburg, M. 1961. Norrie's Disease: A new hereditary bilateral pseudotumour of the
970 retina. Acta Ophthalmologica 399:757-772.
971 Ward, B. J. and C. van Oosterhout. 2016. HYBRIDCHECK: software for the rapid
972 detection, visualization and dating of recombinant regions in genome sequence
973 data. Mol Ecol Resour 16:534-539.
974 Weiss, L. A., S. Purcell, S. Waggoner, K. Lawrence, D. Spektor, M. J. Daly, P. Sklar, and
975 D. Skuse. 2007. Identification of EFHC2 as a quantitative trait locus for fear
976 recognition in Turner syndrome. Hum Mol Genet 16:107-113.
977 Whitman, C. O. 1919. Orthogenic Evolution of Pigeons. Posthumous works of C.O.
978 Whitman. Carnegie Inst., Washington, D.C.
979 Wittkopp, P. J., B. K. Haerum, and A. G. Clark. 2004. Evolutionary changes in cis and
980 trans gene regulation. Nature 430:85-88.
981 Wittkopp, P. J. and G. Kalay. 2012. Cis-regulatory elements: molecular mechanisms and
982 evolutionary processes underlying divergence. Nat Rev Genet 13:59-69.
983 Yamada, T., H. Akamatsu, S. Hasegawa, Y. Inoue, Y. Date, H. Mizutani, N. Yamamoto,
984 K. Matsunaga, and S. Nakata. 2010. Melanocyte stem cells express receptors for
985 canonical Wnt-signaling pathway on their surface. Biochemical and biophysical
986 research communications 396:837-842.
987 Yandell, M., C. D. Huff, H. Hu, M. Singleton, B. Moore, J. Xing, L. B. Jorde, and M. G.
988 Reese. 2011. A probabilistic disease-gene finder for personal genomes. Genome
989 Res 21.
990 Zhang, W., K. K. Dasmahapatra, J. Mallet, G. R. Moreira, and M. R. Kronforst. 2016.
991 Genome-wide introgression among distantly related Heliconius butterfly species.
992 Genome Biol 17:25.
993 Zinn, A. R., H. Kushner, and J. L. Ross. 2008. EFHC2 SNP rs7055196 is not associated
994 with fear recognition in 45,X Turner syndrome. American journal of medical
995 genetics. Part B, Neuropsychiatric genetics : the official publication of the
996 International Society of Psychiatric Genetics 147B:507-509.
997

998 **Figures**

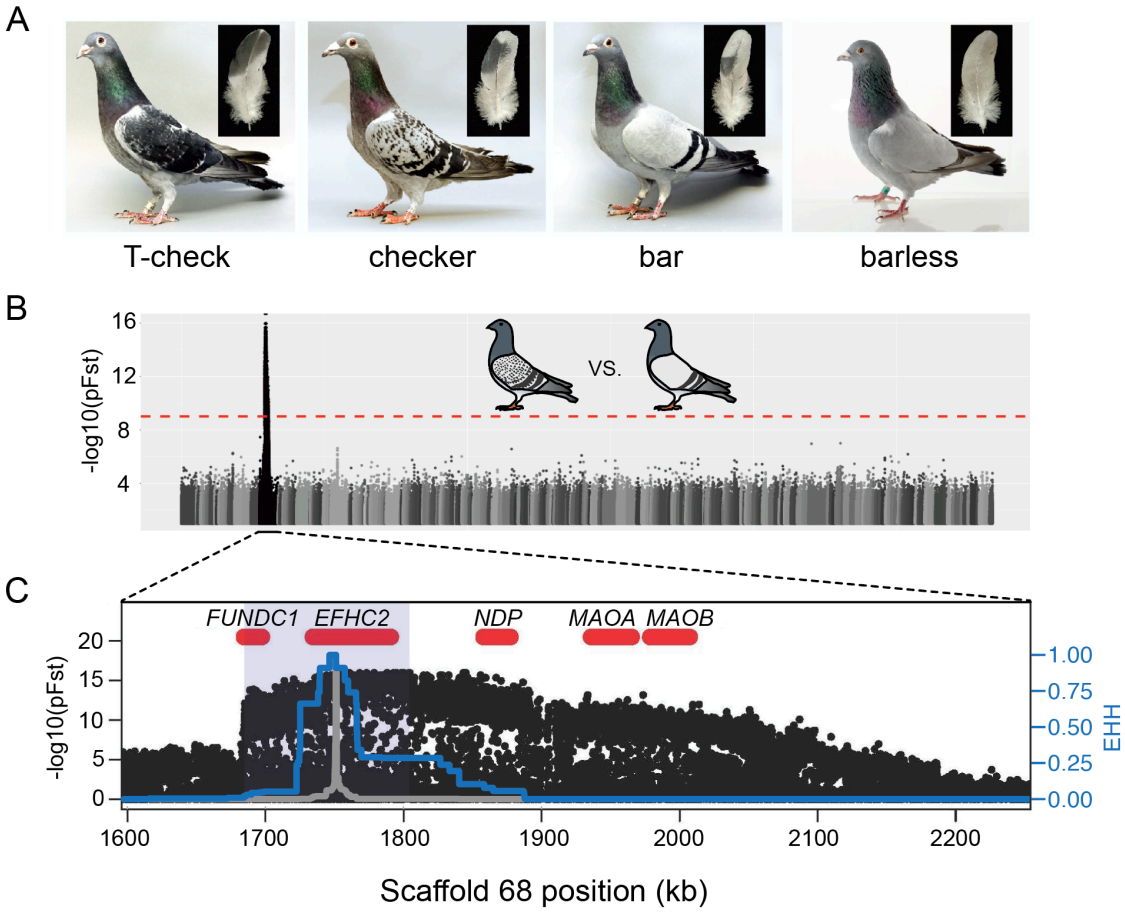

999 **Fig. 1.** A single genomic region is associated with rock pigeon (*C. livia*) wing
1000 pigmentation pattern (A) Four classical wing pattern pigmentation phenotypes, shown in
1001 decreasing order of genetic dominance and melanism (left to right): T-check, checker,
1002 bar, and barless. Photos courtesy of the Genetics Science Learning Center
1003 (http://learn.genetics.utah.edu/content/pigeons). (B) Whole-genome pFst comparisons
1004 between the genomes of bar (n=17) and checker (n=24) pigeons. Dashed red line marks
1005 the genome-wide significance threshold (9.72e-10). (C) Detail of pFst peak shows region
1006 of high differentiation on Scaffold 68. Five genes within the region are shown in red.
1007 Blue shading marks the location of the smallest shared haplotype common to all checker
1008 and T-check birds. Haplotype homozygosity in the candidate region extends further for
1009 checker and t-check birds (blue trace) than for bar birds (gray), a signature of positive
1010 selection for the derived alleles. Extended haplotype homozygosity (EHH) was measured
1011 from focal position 1,751,072 and follows the method of Sabeti et al. (2007).

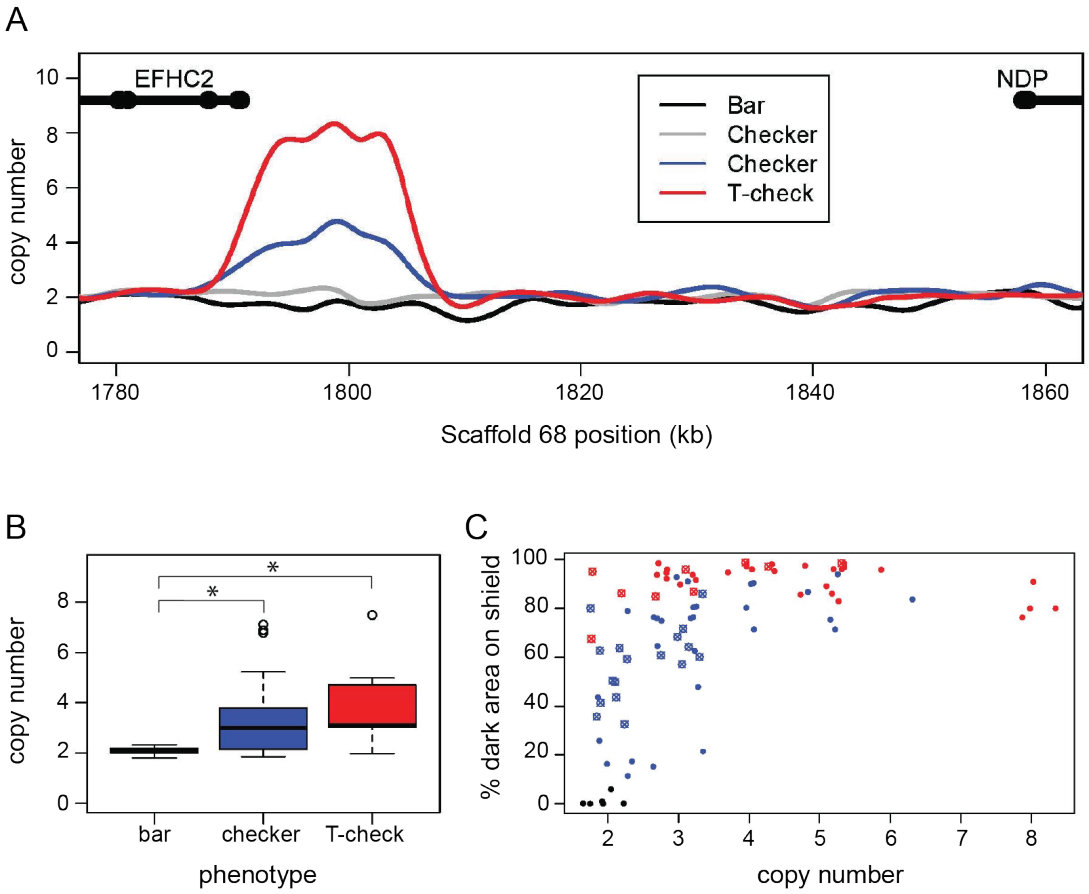

Fig. 2. A copy number variant (CNV) in the candidate region is associated with T-check and checker phenotypes. (A) Normalized read depths from resequenced birds are plotted in the candidate region between *EFHC2* and *NDP* on Scaffold 68. Thickened portions of gene models represent exons and thin portions are introns. Representative individual read depth traces are shown for the following: black for bar *C. livia*, grey for checker *C. livia* individuals without additional copies of the CNV, blue for checker *C. livia* individuals with additional copies of the CNV region, red for T-check *C. livia*. (B) CNV quantification for 94 birds (20 bar, 56 checker, and 18 T-check). Checker and T-check phenotypes (as reported by breeders) were associated with increased copy numbers (p=2.1e-05). (C) CNV and phenotype quantification for an additional 84 birds, including 26 feral pigeons. Increased copy number was associated with an increase in dark area on the wing shield (r^2=0.46, linear regression). Points are colored by reported phenotype and origin: bar, black; checker, blue; T-check, red; domestic breeds, solid points; ferals, cross points.

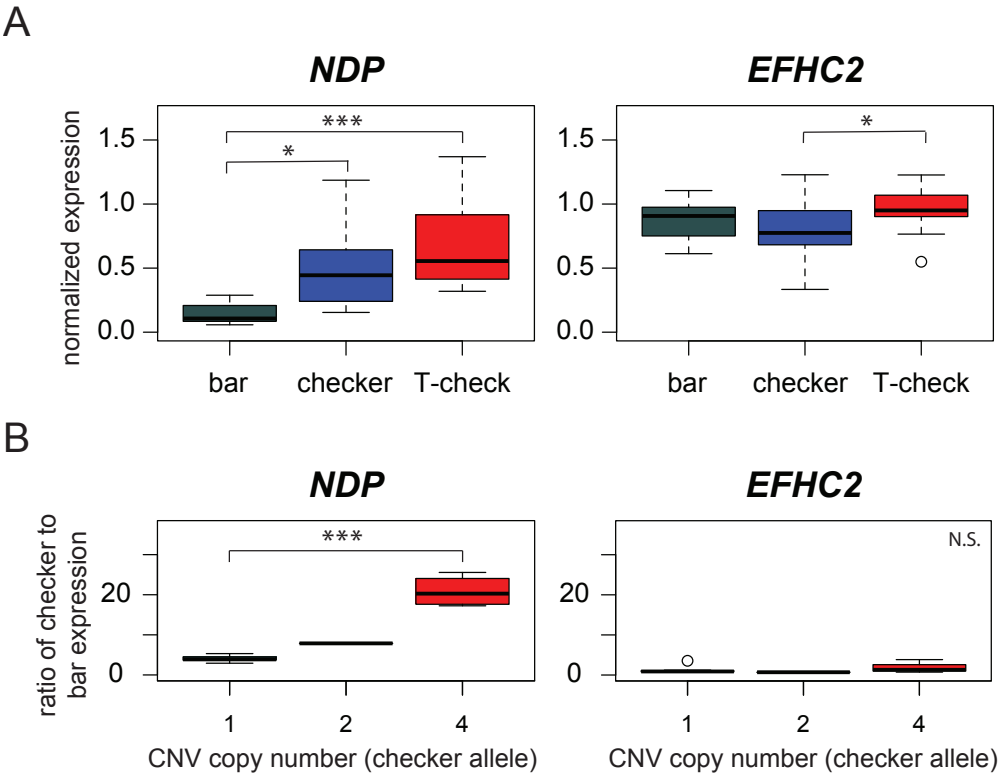

Fig. 3. Expression differences in *NDP*, but not *EFHC2*, indicate *cis*-regulatory differences associated with pigmentation phenotypes. (A) qRT-PCR assays demonstrate higher expression of *NDP* in regenerating feathers of checker and T-check birds than in bar birds. Expression levels of *EFHC2* are indistinguishable between bar and melanistic phenotypes (p=0.19), although checker and T-check differed from each other (p=0.046). (B) Allele-specific expression assay in regenerating feathers from heterozygous bar/checker birds for *NDP* and *EFHC2*. Copies of the CNV region on the checker chromosome were quantified using a custom Taqman assay. Boxes span the first to third quartiles, bars extend to minimum and maximum observed values, black line indicates median. Expression of *EFHC2* alleles were not significantly different, and checker alleles of *NDP* showed higher expression than the bar allele; p=0.0028 for two-sample t-test between 1 vs. 4 copies, p=1.84e-06 for glm regression.

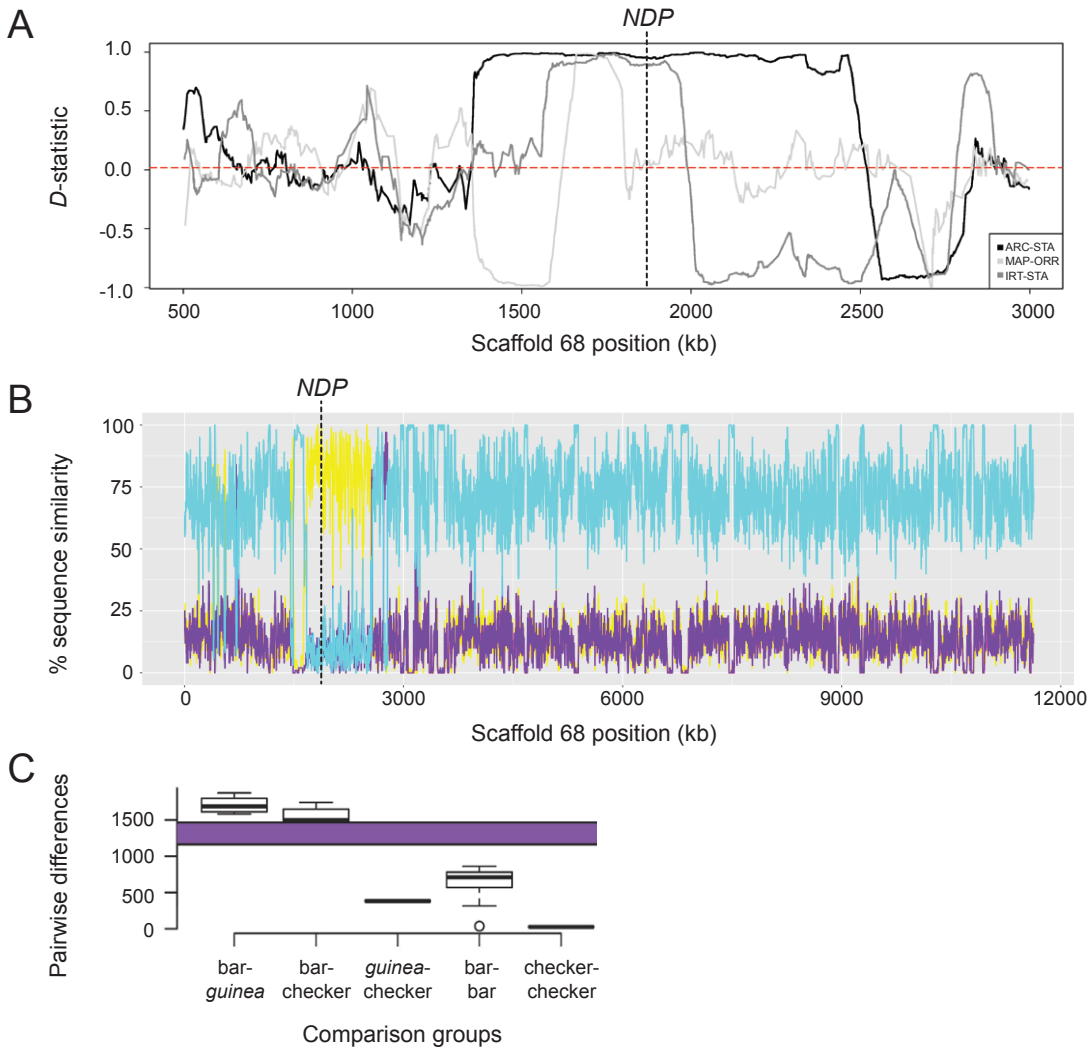

Fig. 4. Signatures of introgression of the checker haplotype from *C. guinea* to *C. livia*. (A) ABBA-BABA test with *C. livia* (bar), *C. livia* (checker), *C. guinea*, and *C. palumbus* shows elevated D-statistic in the Scaffold 68 candidate region. Three representative ABBA-BABA tests are shown and dashed red line marks the genome-wide mean *D*-statistic for 10 X 10 different combinations of bar and checker birds (ARC-STA, MAP-ORR, IRT-STA are shown, see Methods). (B) HybridCheck shows sequence similarity between three pairwise comparisons: representative bar (Fer_VA), checker (ARC), and *C. guinea* individuals. (C) Expected (purple bar) and observed SNP differences in the minimal haplotype region for different pairwise comparisons between and among bar, checker, and *C. guinea*.

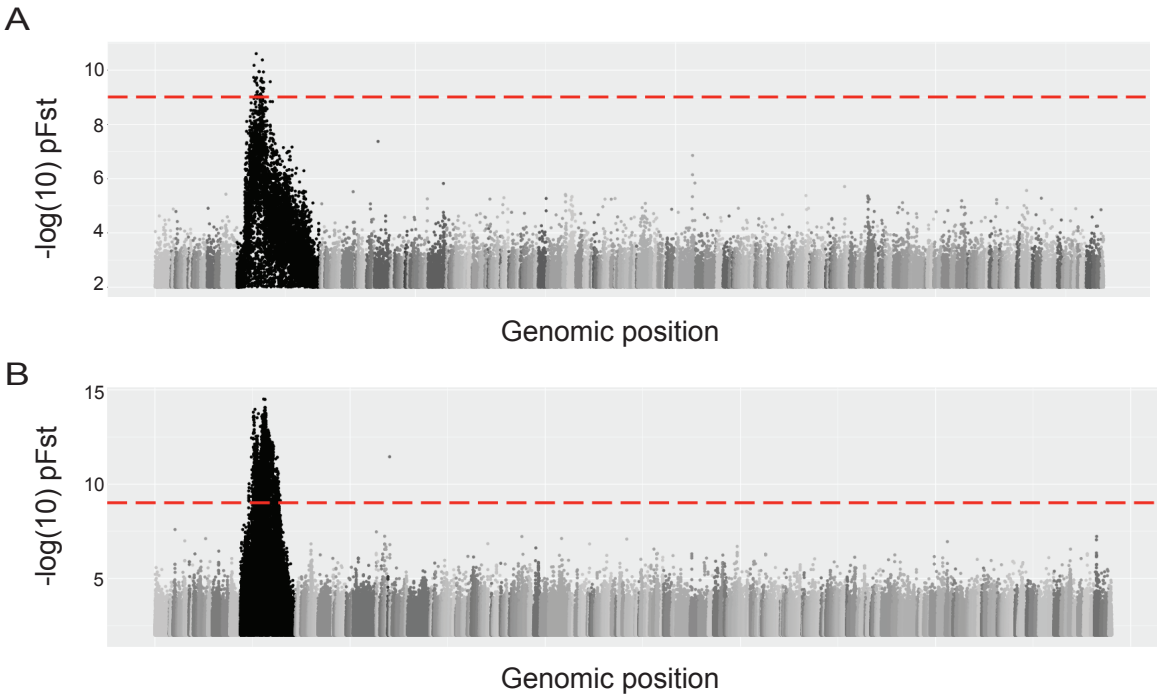

1052

1053 **Fig. S1.** Whole genome pFst comparisons to identify a candidate genomic region
1054 differentiated between birds with different wing pattern phenotypes. (A) Whole genome
1055 pFst comparing 32 bar and 27 checker and T-check birds. (B) Whole genome pFst
1056 comparing 32 bar and 9 barless birds.

1057

1058

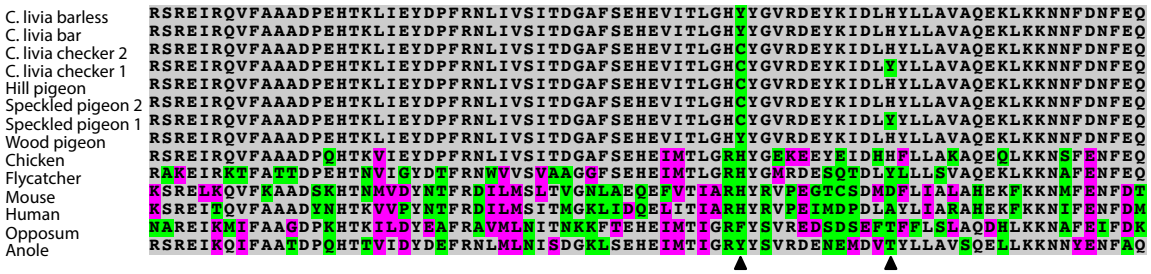

Fig. S2. EFHC2 amino acid sequences of pigeons and other amniotes (residues 525-604). Variable amino acid residues are marked in magenta (similar residues) and green (different residues). Checker *C. livia*, *C. rupestris*, and *C. guinea* share 572C while bar *C. livia* are fixed for 572Y (left arrowhead). Checker *C. livia* and *C. guinea* are polymorphic for 584H/Y (right arrowhead).

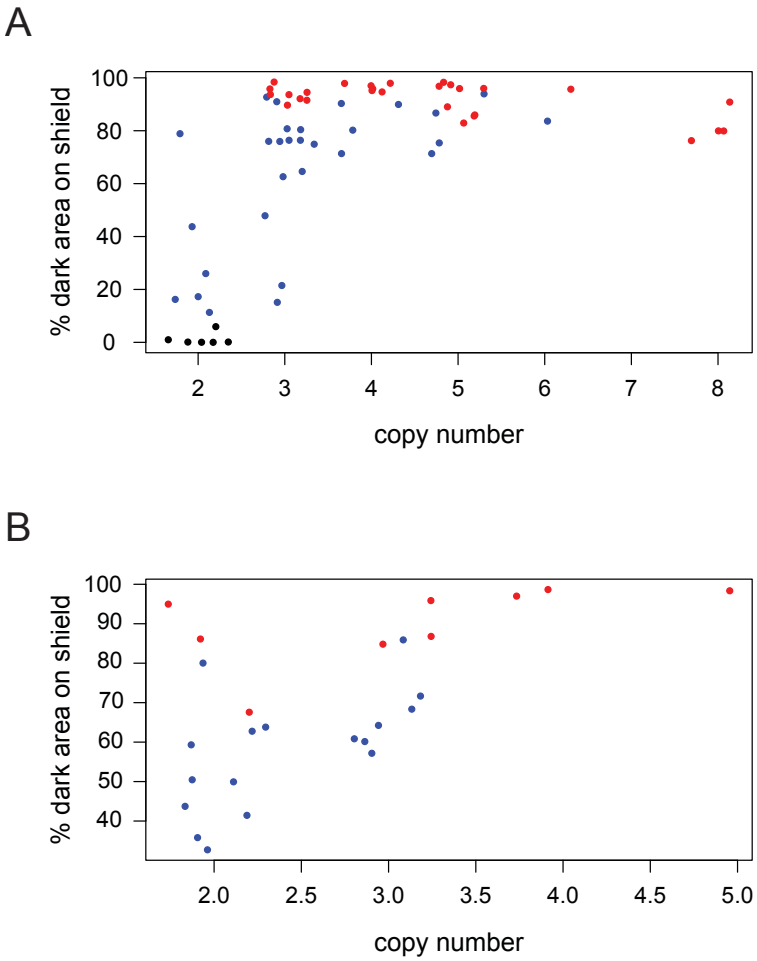

1066

1067

1068 **Fig. S3.** CNV is associated with darker wing shield pigmentation. CNV and phenotype
1069 quantification for (A) domestic breeds (n=58) and (B) wild-caught ferals (n=26), parsed
1070 from data in Fig. 2C.

1071

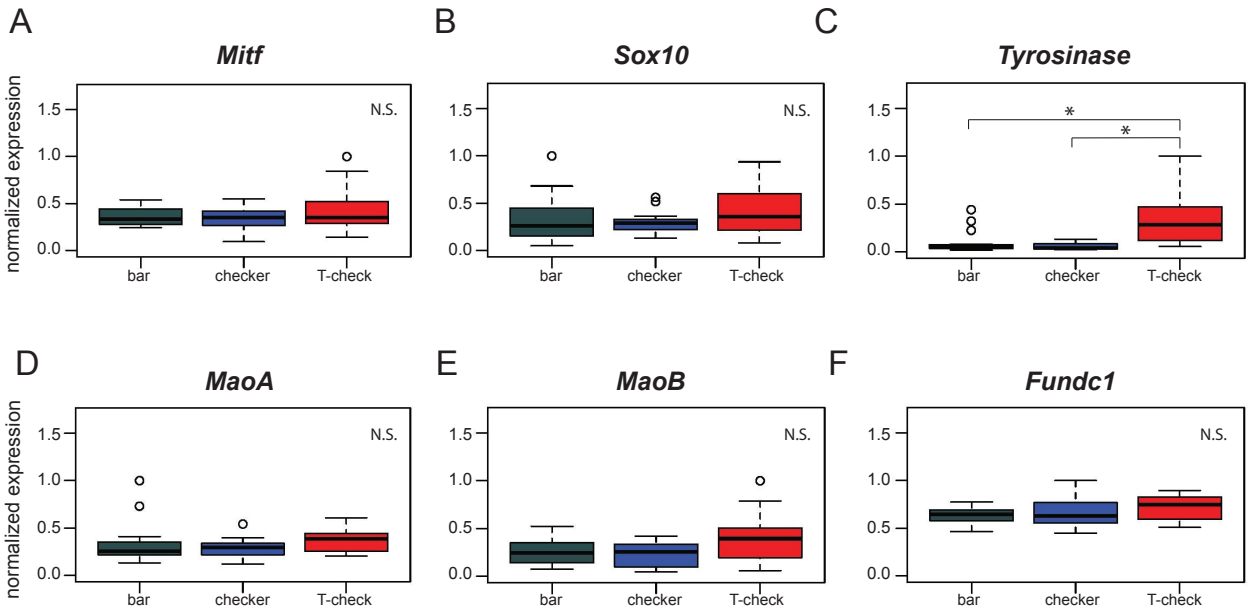

Fig. S4. Expression of genes involved in pigmentation and genes in the candidate region. Expression levels of *Mitf* (A), *Sox10* (B), *MaoA* (D), *MaoB* (E), and *Fundc1* (F) are indistinguishable across phenotypes. (C) *Tyrosinase* shows increased expression in T-check birds relative to bar (p=2.4e-04) and checker birds (p=3.8e-05). Boxes span the first to third quartiles, bars extend to minimum and maximum observed values, black line indicates median. Expression values are analyzed by Pairwise Wilcoxon test (p-value adjustment method: fdr).

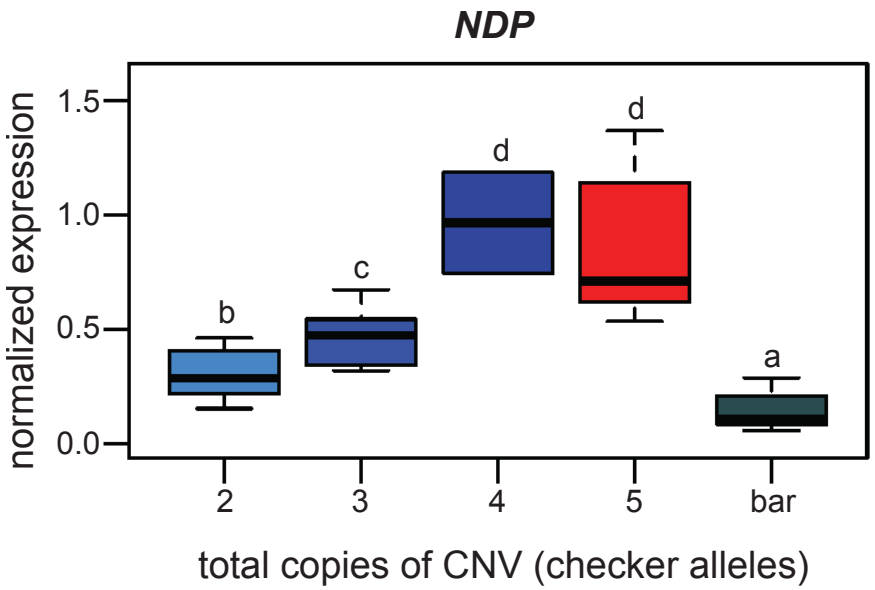

Fig. S5. *NDP* expression varies by copy number and phenotype. qRT-PCR expression assay for *NDP* (Fig. 3A) is parsed by copy number in the CNV region. All checker (blue) and T-check (red) birds, except for the single individual with four total copies (dark blue), are heterozygous for bar. Increase in *NDP* expression is correlated with increasing numbers of copies of the CNV region. Boxes span the first to third quartiles, bars extend to minimum and maximum observed values, black line indicates median. Different letters indicate significant pairwise differences. Pairwise Wilcoxon test (p-value adjustment method: fdr) results by copy number: 2-3 copies, p=0.03788; 2-4 copies, p=0.04938; 2-5 copies, p=0.00015; 2 copies-bar, p=0.00432; 3-4 copies, p=0.03788; 3-5 copies, p=0.00122; 3 copies-bar, p=1.9e-06; 4-5 copies, p=0.48485; 4 copies-bar, p=0.02179; 5 copies-bar, p=1.9e-06.

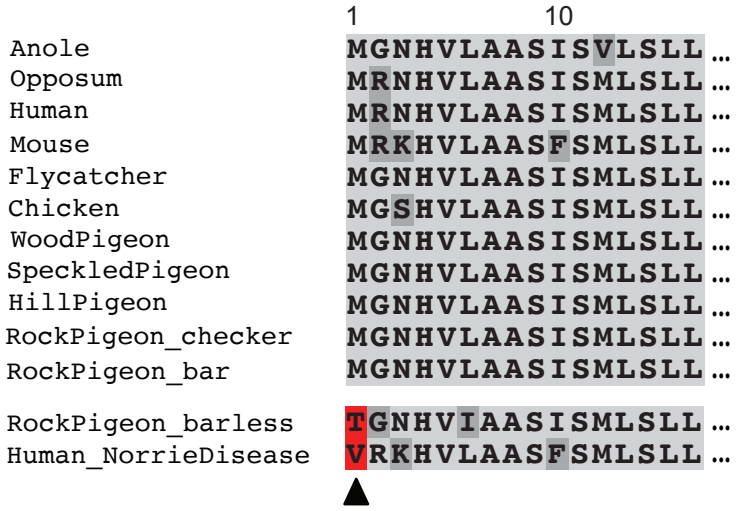

Fig. S6. Barless pigeons have a nonsense mutation at the highly-conserved translation start site of *NDP*. Barless rock pigeons are homozygous for a nonsense mutation that truncates the amino terminus of *NDP* to 13 amino acids; the same amino acid position is affected by a mutation in two human families with hereditary blindness (red, bottom of alignments).

Fig. S7. Speckled pigeon (*Columba guinea*). Photo courtesy of Kjeuring (CC BY 3.0 license, https://creativecommons.org/licenses/by/3.0/legalcode). Photo cropped from "speckled pigeon *Columba guinea* Table Mountain Cape Town," https://en.wikipedia.org/wiki/Speckled_pigeon#/media/File:Speckledpigeon.JPG. Inset feather image by the authors.